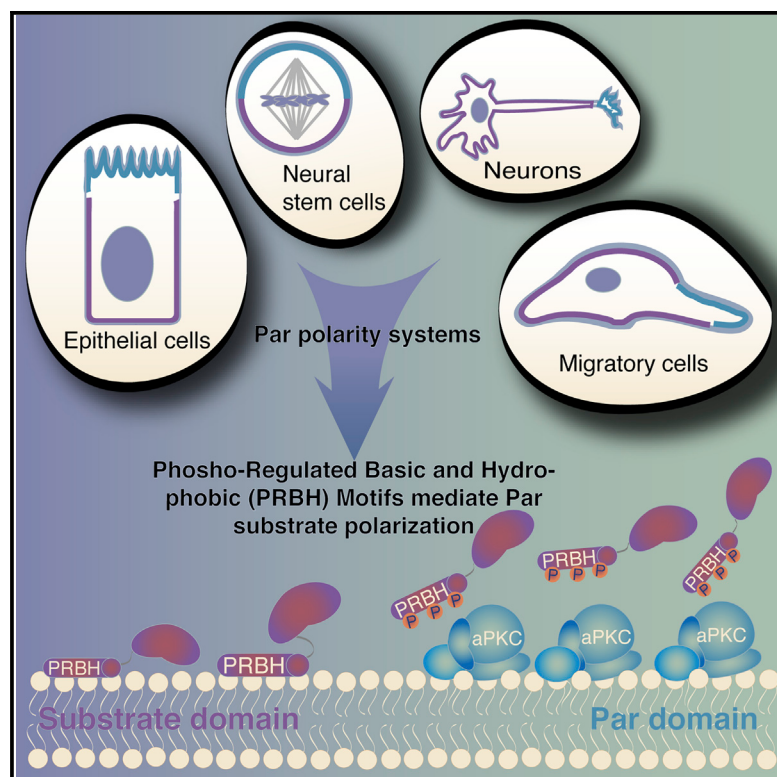


Developmental Cell

Establishment of Par-Polarized Cortical Domains via Phosphoregulated Membrane Motifs

Graphical Abstract



Authors

Matthew J. Bailey, Kenneth E. Prehoda

Correspondence

prehoda@uoregon.edu

In Brief

The mechanism of Par substrate localization and polarization has remained elusive. Bailey and Prehoda identify a phosphorylation-regulated motif that mediates cortical localization and also aPKC-mediated displacement of diverse Par substrates from the cortex. A bioinformatic screen demonstrates that candidate phosphoregulated membrane-association motifs are common in animal proteomes.

Highlights

- Diverse Par complex substrates directly bind phospholipids
- aPKC phosphorylation neutralizes substrate lipid binding
- Phosphorylation-induced displacement excludes substrates from Par cortical domain
- Many candidate phosphoregulatory motifs are present in animal proteomes

Establishment of Par-Polarized Cortical Domains via Phosphoregulated Membrane Motifs

Matthew J. Bailey¹ and Kenneth E. Prehoda^{1,*}

¹Department of Chemistry and Biochemistry, Institute of Molecular Biology, University of Oregon, Eugene, OR 97403, USA

*Correspondence: prehoda@uoregon.edu

<http://dx.doi.org/10.1016/j.devcel.2015.09.016>

SUMMARY

The Par polarity complex creates mutually exclusive cortical domains in diverse animal cells. Activity of the atypical protein kinase C (aPKC) is a key output of the Par complex as phosphorylation removes substrates from the Par domain. Here, we investigate how diverse, apparently unrelated Par substrates couple phosphorylation to cortical displacement. Each protein contains a basic and hydrophobic (BH) motif that interacts directly with phospholipids and also overlaps with aPKC phosphorylation sites. Phosphorylation alters the electrostatic character of the sequence, inhibiting interaction with phospholipids and the cell cortex. We searched for overlapping BH and aPKC phosphorylation site motifs (i.e., putative phosphoregulated BH motifs) in several animal proteomes. Candidate proteins with strong PRBH signals associated with the cell cortex but were displaced into the cytoplasm by aPKC. These findings demonstrate a potentially general mechanism for exclusion of proteins from the Par cortical domain in polarized cells.

INTRODUCTION

Animal cells are polarized in remarkably diverse ways, such as the specialized apical cortex of a simple epithelium and the leading edge of motile cells (Knoblich, 2010; Overeem et al., 2015; Tepass, 2012). Although these cells are dramatically different, they are polarized by the same molecular machinery known as the Par complex (Goehring, 2014; Goldstein and Macara, 2007). The capacity of the Par complex to direct diverse cell polarities derives in part from its ability to act on a multitude of downstream proteins. For example, in asymmetrically dividing neural stem cells, the Par complex polarizes fate determinants (Betschinger et al., 2003; Knoblich, 2010), whereas in epithelia it organizes junctional components (Suzuki et al., 2001; Tepass, 2012). The characteristic adaptability of the Par complex to regulate distinct classes of proteins suggests that there may be a common mechanism by which it acts on downstream factors, yet little is known about how Par activity is coupled to substrate polarity. Knowledge of this mechanism is important not only for our basic understanding of Par-mediated polarity, but it might also allow for the identification of novel Par-regulated proteins and provide insight into the evolutionary pathways underlying the wide range of polarities found among metazoa.

The Par complex polarizes cells by creating and maintaining mutually exclusive cortical domains. Upstream factors that can be cell-type-specific define the Par domain (Cuenca et al., 2003; Harris and Peifer, 2005; Martin-Belmonte et al., 2007; Rolls et al., 2003; Schober et al., 1999; Wodarz et al., 1999), and downstream proteins are excluded from this cortical area to create the substrate domain. While the Par complex can function through other mechanisms (Cline and Nelson, 2007; von Stein et al., 2005; Zhang and Macara, 2006), a key output is the activity of atypical protein kinase C (aPKC). Proteins that are directly downstream of the Par complex are often aPKC substrates, and phosphorylation is both necessary and sufficient for cortical displacement and concomitant removal from the Par domain (Atwood and Prehoda, 2009; Betschinger et al., 2003; Hao et al., 2006; Hurov et al., 2004; Smith et al., 2007; Suzuki et al., 2004; Wirtz-Peitz et al., 2008; Zhang et al., 2001). For proteins polarized by this mechanism, their phosphorylation must be coupled to release from the cortex. Although phosphorylation-coupled cortical release is critical to Par complex-mediated polarity, very little is known about the mechanisms by which Par substrates associate with the cortex and how phosphorylation is linked to this interaction. The lack of sequence homology or shared globular domain structure among Par substrates has made it difficult to identify a “polarity code.”

The Par complex functions at the cell cortex, a complex organelle that includes the phospholipid bilayer and a meshwork of membrane-associated proteins and cytoskeletal elements beneath it (Engelman, 2005; Groves and Kuriyan, 2010; Morone et al., 2006). It has been unclear how these components might contribute to Par-mediated polarity, although actin polymerization is known to be required and protein-protein interactions have been implicated for certain substrates (Betschinger et al., 2005; Dho et al., 1999; Knoblich et al., 1997; Strand et al., 1994). Direct lipid binding has only been demonstrated for Numb PTB domain, however, this is not sufficient for cortical localization (Dho et al., 1999). Given the complexity of the cell cortex and the potential for diverse protein-phospholipid and protein-protein interactions, we set out to identify the interactions that retain Par-polarized proteins within their cortical domain and how aPKC phosphorylation regulates these cortical interactions to prevent entry into the Par domain.

RESULTS

Short, Charged, Hydrophobic Motifs Target Lgl, Mira, and Numb to the Cell Cortex

To determine if there might be a general mechanism of Par complex polarization, we selected three substrates with no

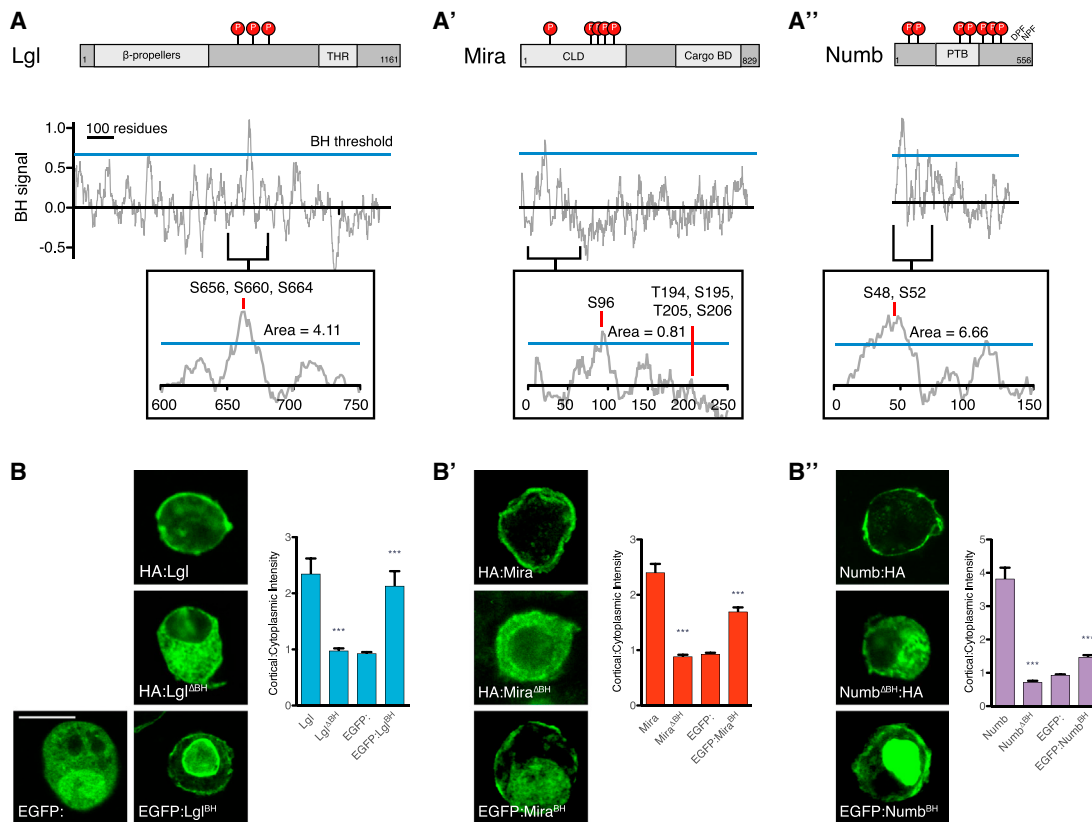


Figure 1. Lgl, Mira, and Numb Localize to the Cell Cortex through BH Motifs

(A–A'') Basic hydrophobic motif signal in Lgl (A), Mira (A'), and Numb (A''). Previous work identified domains with multiple potential cortical targeting domains in Lgl, Mira, and Numb. The BH-search algorithm was used to analyze the sequences of *Drosophila* Lgl, Mira, and Numb. The BH signal is shown across each protein's domain architecture. BH motifs are defined by peaks with a BH signal >0.6 (denoted by blue line) and the peak area indicates the strength of the peak's BH character. Each protein has a single BH motif that contains at least one aPKC phosphorylation site. THR, tomosyn homology region; CLD, cortical localization domain; Cargo BD, cargo binding domain; PTB, phosphotyrosine binding domain; DPF, α -adaptin-binding motif; NPF, Eps15-binding motif. (B–B'') BH motifs are necessary and sufficient for cortical targeting of Lgl (B), Mira (B'), and Numb (B''). Deletion constructs were used to determine if the BH motif is necessary and sufficient for localization to the S2 cell cortex. Representative images of the localization are presented for each protein when transiently transfected in S2 cells and characterized by either immunofluorescence for the HA epitope tag or by EGFP fluorescence. Localization to the cell cortex was quantified as an intensity ratio for the cortex versus the cytoplasm. At least 17 cells were quantified and the mean and the SEM are shown. Asterisks indicate $p < 0.0001$ as assessed by a t test to compare each Δ BH construct to its respective full-length control or each EGFP-fusion to its EGFP control. Scale bar, 10 μ m.

apparent sequence homology or shared domain structure: Lgl, Mira, and Numb (Figures 1A–1A'') (Betschinger et al., 2005; Dho et al., 2006; Fuerstenberg et al., 1998; Matsuzaki et al., 1998). Lgl and Numb each have protein interaction domains: β -propellers, a tomosyn homology region (THR), and a phosphotyrosine-binding (PTB) domain, but they are not sufficient for cortical association in *Drosophila* (Betschinger et al., 2005; Knoblich et al., 1997). Cortical localization of Mira is specified by its NH₂-terminal 1–290 amino acids (Fuerstenberg et al., 1998; Matsuzaki et al., 1998), which does not contain any recognizable globular domains. These three diverse Par complex substrates lack clear globular domains that would mediate interactions with the cortex or membrane (Lemmon, 2008). Short stretches of basic and hydrophobic (BH) amino acids are known to interact with the membrane, so we analyzed the basic and hydrophobic character of the sequences using the BH scoring algorithm (Brzeska et al., 2010). Sequence windows with BH scores exceeding 0.6 are

candidate phospholipid binding motifs and we found that Lgl, Mira, and Numb each contain a single region above this threshold (Figures 1A–1A''). Interestingly, each of these sequences overlaps with a known or predicted aPKC phosphorylation site (Atwood and Prehoda, 2009; Betschinger et al., 2003; Smith et al., 2007). We identified several aPKC sites with BH scores below the threshold, indicating that not all aPKC sites are BH motifs (see below for a more extensive comparison of BH motifs and the aPKC recognition sequence).

Given their short sequences, the BH scoring algorithm could have a high false positive rate, so we investigated whether the Lgl, Mira, and Numb BH motifs mediate cortical localization. Each of these proteins localizes to the cortex of cultured *Drosophila* S2 cells consistent with their ability to interact with the cortex opposite Par domains. Deletion of each protein's candidate BH motif caused a loss of cortical enrichment and strong cytoplasmic signal (Figures 1B–1B''). In some cases, BH

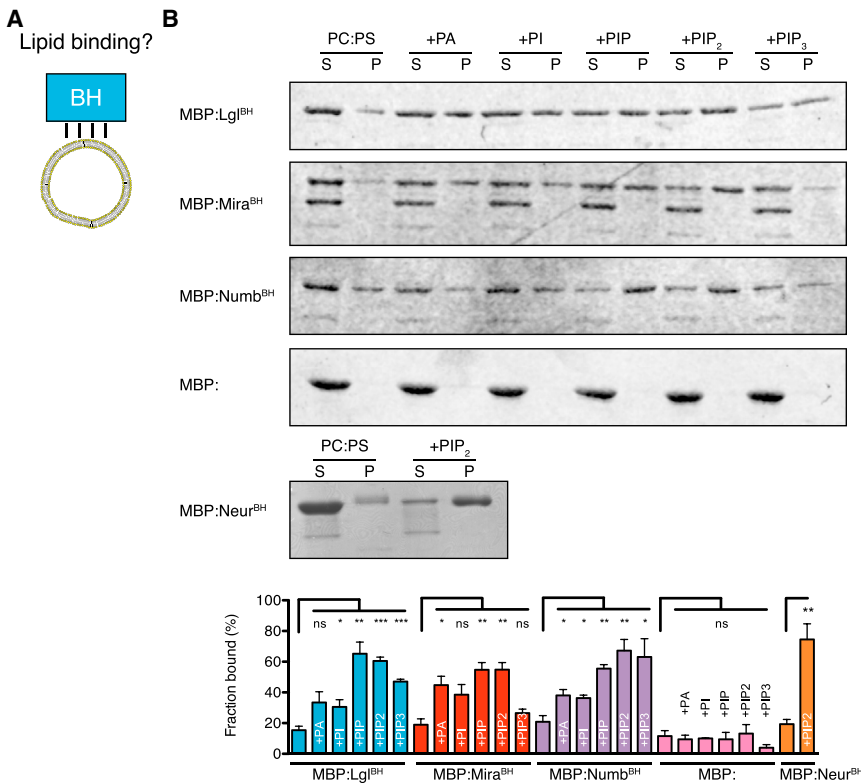


Figure 2. Phospholipid Binding Mediates Localization to the Cell Cortex

(A) BH motif phospholipid binding was tested using a cosedimentation phospholipid binding assay.

(B) The BH motifs of Lgl, Mira, and Numb bind directly to phospholipid vesicles. A representative Coomassie-stained SDS-PAGE gel from a lipid vesicle-binding cosedimentation assays is presented. Each protein was characterized with an NH₂-terminal maltose binding protein (MBP) fusion. The BH motif from Neuralized (Neur residues 68–88) was used as a positive control. The supernatant (S) and pellet (P) contain the unbound and bound fractions, respectively. All vesicles contained a 4:1 mixture of 1,2-dioleoyl-sn-glycero-3-phosphocholine (PC) to 1,2-dioleoyl-sn-glycero-3-[phospho-L-serine] (PS). Lanes marked by +X contained a third lipid that was added to be 10% of the total lipid by mass. PA, L- α -phosphatidic acid; PI, L- α -phosphatidylinositol; PI4P, L- α -phosphatidylinositol-4-phosphate; PIP₂, phosphatidylinositol-4,5-bisphosphate; PIP₃, 1,2-dioleoyl-sn-glycero-3-[phosphoinositol-3,4,5-trisphosphate]. The fraction bound expressed as a percentage is shown in the bottom panel. Error bars represent SEM from three independent measurements. Significance levels, *p < 0.05, **p < 0.01, and ***p < 0.001.

See also Figure S1 for sequence analysis of Neur BH motif.

motifs often require additional multivalent interactions to associate with the membrane (Papayannopoulos et al., 2005; Swierczynski and Blackshear, 1996; Winters et al., 2005), so we tested whether each could function on their own. When EGFP is attached to stabilize these short, unstructured sequences (~30–70 amino acids), each BH motif was enriched at the S2 cortex (Figures 1B–1B''), although at reduced levels compared to the full-length proteins. These data indicate that cortical localization of Lgl, Mira, and Numb is mediated by their BH motifs. Although additional interactions are likely needed to reinforce cortical recruitment, this appears to be a common mechanism for BH-mediated membrane association (McLaughlin and Murray, 2005; Rohatgi et al., 1999; Winters et al., 2005).

Lgl, Mira, and Numb BH Motifs Bind Directly to Phospholipids

The key role of the Lgl, Mira, and Numb BH motifs in cortical localization suggests that protein-phospholipid interactions are, at least in part, responsible for the cortical association of Par substrates. To test for direct protein-phospholipid interactions, we purified the BH motifs as maltose-binding protein (MBP) fusions and tested whether they associate with giant unilamellar vesicles (GUVs) of various lipid compositions via a co-sedimentation assay (Figure 2A). Using the BH motif from Neuralized (Neur) as a positive control (Skwarek et al., 2007), we found that each of the BH motifs from Lgl, Mira, and Numb exhibited very little binding to vesicles containing phosphatidylserine and phosphatidylcholine alone, but interacted with these vesicles when they were doped with various negatively charged phospholipids (Figures 2B and S1). Although phosphoinositides

with multiple phosphates were slightly preferred over other negatively charged lipids (e.g., phosphatidic acid [PA]), the level of specificity is small enough that we do not expect it to be physiologically relevant.

Par Substrate Cortical Recruitment Is Mediated by Electrostatic Interactions

The BH motifs of Lgl, Mira, and Numb have multiple positively charged residues that may confer favorable electrostatics for binding phospholipids. Polybasic regions can bind negatively charged phospholipids, including PS and phosphoinositides. To investigate the role of charge in cortical targeting, we mutated basic residues within the BH motif to the acidic residue aspartic acid; these mutations reduced the calculated BH signal to often eliminate BH motif identification (Figures 3A–3B''). We found that mutations that acidify the BH motif greatly reduce cortical localization of the full-length protein in S2 cells (Figures 3C–3D''). Further, this effect was not site-specific because mutations at multiple sites along the BH motif caused similar localization phenotypes (Figure S2A).

Consistent with their effect on cortical localization, charge swap mutations reduced BH affinity for liposomes (Figures 3E–3F''). To further test the role of electrostatics, we measured liposome interactions in the presence of 500 mM KCl, which reduces the entropic cost of displacing ions from the bilayer surface (McLaughlin, 1989). High ionic strength reduced the interaction between phospholipids and each BH motif (Figure S2B), supporting the conclusion that direct, electrostatic interactions with phospholipids mediate BH motif cortical enrichment.

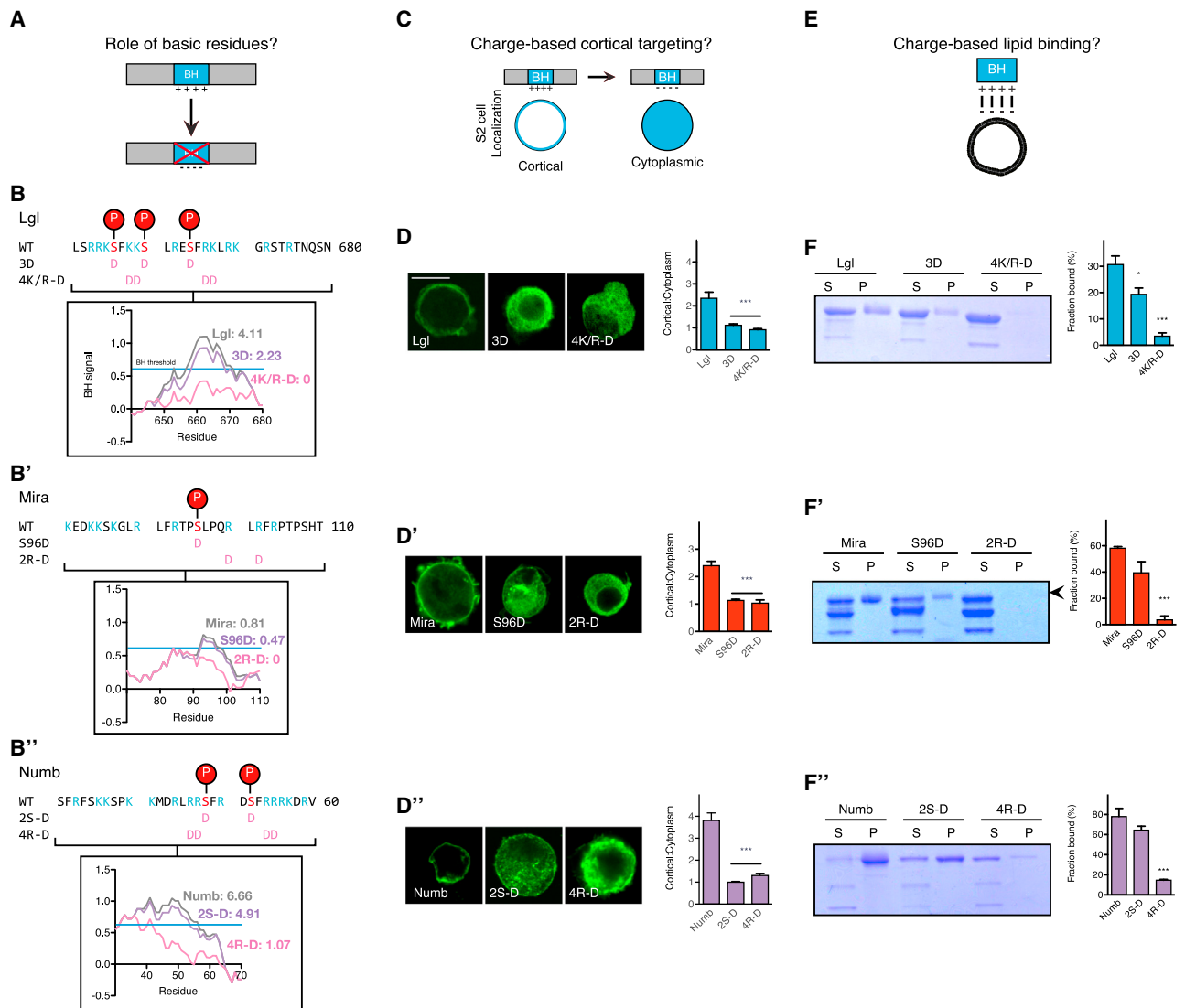


Figure 3. Electrostatic Interactions Mediate Lgl, Mira, and Numb Interactions with Phospholipids and the Cell Cortex

(A) BH motif point mutants test the role for charged residues in cortical localization.

(B–B'') Charged residues contribute to BH motif of Lgl (B), Mira (B'), and Numb (B''). The sequence of the BH motifs from Lgl, Mira, and Numb are displayed, highlighting basic residues (blue) and aPKC phosphorylation sites (red). Terminology and location of the point mutants are displayed with pink aspartic acids. The inset shows the effect of each mutation on the BH signal and the area of the BH peak, as computed by BH-search. The BH threshold is displayed by a blue line with a BH signal of 0.6.

(C) S2 cell localization assay tested if BH motif charge mediates localization to the cell cortex.

(D–D') Mutations to acidic residues reduce localization to the cell cortex in transiently transfected S2 cells. The localization of each full-length protein with point mutations was characterized by immunostaining for the HA epitope tag (located on each protein's NH₂ terminus), and the localization was quantified as a cortical to cytoplasmic signal intensity ratio for at least 16 cells (mean ± SEM). Scale bar, 10 μm. See also Figure S2A for additional point mutants.

(E) Lipid binding assays tested if BH motif charge disrupts phospholipid binding.

(F–F'') Acidic mutations reduce phospholipid binding. A Coomassie-stained gel from lipid vesicle binding sedimentation assays with vesicles of 4:1 PC:PS plus 10% PIP₂ is shown. S indicates supernatant and P the pellet fraction. Arrowheads mark the full MBP-BH protein while other bands are truncation products (e.g., MBP alone). The fraction of protein bound, quantified as the amount of protein in the pellet over total protein, was quantified in triplicate for each vesicle composition. The mean and SEM of the fraction bound are shown. *p < 0.05, **p < 0.0001. Significance was evaluated using a non-parametric t test relative to the unmutated BH motif.

See also Figure S2.

aPKC Phosphorylation Regulates BH Cortical Targeting and Phospholipid Binding

The Lgl, Mira, and Numb BH motifs contain verified and/or predicted aPKC phosphorylation sites. As charge swap mutations

significantly reduce BH motif phospholipid binding and cortical association, we predicted that Par-induced polarization results when BH and aPKC phosphorylation site motifs are in close enough proximity that the phosphorylation(s) can sufficiently

influence BH electrostatics to reduce the affinity for the membrane. This would allow Par substrates to associate with the cortex via their BH motif (and any accessory interactions) in regions lacking the Par complex. However, upon entering the Par cortical domain, the BH motif would be phosphorylated by aPKC, altering electrostatic character and reducing membrane affinity. Consistent with this model, we observed that phosphomimetic Lgl BH had reduced PIP₂ binding, although no statistically significant difference was observed for Mira or Numb BH motifs (Figures 3F–3F"). However, expression of aPKC significantly reduced cortical enrichment of the motifs from all three proteins (Figures 4A–4B"), recapitulating the behavior of the full-length proteins. Non-phosphorylatable variants of each BH motif remain localized to the cell cortex when aPKC was expressed (Figures 4B–4B" and S3A), indicating that phosphorylation is required for displacement. Furthermore, we found that aPKC phosphorylation inhibits BH interaction with PIP₂-containing vesicles, suggesting that disruption of this direct interaction is responsible for cortical displacement (Figures 4C–4D"). Addition of aPKC had no effect on non-phosphorylatable BH motif variants Lgl3A, MiraS96A, or NumbS48AS52A, in the absence of ATP, or with aPKC harboring a kinase dead mutation (K293W) (Figures S3B–S3D). The difference between the phosphomimetic and aPKC-phosphorylated proteins in binding PIP₂-containing vesicles likely arises from the higher negative charge density of the phosphorylated proteins. We conclude that aPKC displaces Lgl, Mira, and Numb from the cortex by phosphorylation inhibiting phospholipid binding.

A Bioinformatics Approach to Identifying Candidate PRBH Motifs

Our analysis of Lgl, Mira, and Numb suggests that phosphoregulated BH (PRBH) motifs mediate Par substrate polarization by coupling phosphorylation to membrane affinity. This coupling derives from the overlap of BH and aPKC phosphorylation motifs, and we used this criterion to search for putative PRBH motifs. We implemented an algorithm in the Python programming language (van Rossum, 2001) using the maximum BH score within a motif (Brzeska et al., 2010) along with a scoring system based on the aPKC phosphorylation site motif consensus sequence (Wang et al., 2012), modified to include Miranda (Figure 5A). We used the maximum BH score rather than the sum of BH scores within a motif to select for short, highly charged sequences like those found in Lgl, Miranda, and Numb. Additionally, to account for the observation that these sequences often contain multiple phosphorylation sites (Graybill and Prehoda, 2014), the PRBH score is increased by 0.2 times the number of phosphorylation sites. The weighting factor was set such that the BH and aPKC site score contributions to the overall PRBH score remained balanced. We used this algorithm to identify candidate PRBH motifs in several animal proteomes and numerically describe PRBH motifs by a maximum BH score (a metric of the basic character), aPKC site scores, and the number of aPKC sites identified (Figures 5B, 5C, S4A, and S4B; Table S1). The Lgl PRBH was identified as one of the top scoring motifs in the proteomes of human, fly, worm, and sponge, demonstrating that its charge and phosphosites are conserved in metazoan (Figures 5B, 5C, and S4A; Table S1). The algorithm also identified Numb and Mira, although with lower PRBH scores. It is important

to note that for two reasons Par-polarized proteins likely represent a subset of PRBH-containing proteins. First, polarity is only one cellular process for which phosphorylation regulated membrane association is important. Second, as many kinases have overlapping specificity it is unlikely that all the identified PRBH motifs are solely aPKC substrates (especially those with low aPKC site scores). For example, two bona fide PRBH proteins regulated by the conventional PKC were identified: MARCKS and diacylglycerol kinase (DGK) (Luo et al., 2003; Topham et al., 1998; Überall et al., 1997). Finally, aPKC functions in other processes besides polarity (Farese et al., 2014; Standaert et al., 2001). While these effects increase the false positive rate for identifying polarity proteins, they also suggest that the algorithm will have utility outside of polarity.

To validate the algorithm, we selected several candidate PRBH motifs to determine if they are bona fide regulated membrane association elements. We selected candidates from the fly and human proteomes with a range of PRBH scores, aPKC site scores, and maximum BH scores (Figures 5B and 5C) to examine how well PRBH score correlates with activity. For each candidate, we tested if they can be phosphorylated by aPKC in vitro, whether they associate with the cortex in S2 cells, and whether aPKC can displace them into the cytoplasm. We found that each protein was indeed phosphorylated by aPKC in an in vitro kinase assay (Figure 5D). Membrane-associated guanylate kinase (MAGUK) p55 subfamily member 7 (MPP7) regulates tight junction formation (Stucke et al., 2007) and has a single, highly scored putative PRBH motif that includes two predicted aPKC phosphosites (Figures 5C and 5E). The candidate MPP7 PRBH was highly enriched at the cell cortex and aPKC expression inhibited cortical localization (Figure 5E). PIP82, a *Drosophila* protein involved in signal transduction downstream of photoreceptors (Suri et al., 1998), similarly contains two PRBH motifs, the stronger of which has high BH character and two predicted aPKC sites (Figures 5B and 5F). We observed that the PIP82 candidate PRBH sequence also localized to the S2 cell cortex and this localization was antagonized by aPKC (Figure 5F).

We also examined several lower scoring PRBH motifs to determine if they function as aPKC regulated cortical localization motifs. The putative PRBH motif on human casein kinase I γ (CKI γ -2) contains a strongly predicted aPKC site rated similar to MPP7, but has weak basic character as demonstrated by a low maximum BH height (Figures 5C and 5G). To our knowledge, its localization remains uncharacterized in polarized cells, but the Casein Kinase-associated protein Lrp6 localizes basolaterally in the *Xenopus* neuroectoderm (Davidson et al., 2005; Huang and Niehrs, 2014). CKI γ -2 PRBH localizes weakly to the cell cortex and has punctate localization suggesting it localizes to endomembrane organelles, as seen previously for Casein kinase (Tomishige et al., 2009). Expression of aPKC reduced the cortical localization of the CKI γ -2 candidate PRBH and did not alter the distribution of CKI γ -2 between the cortex and cytoplasm (Figure 5G). The human tumor suppressor Adenomatous polyposis coli membrane recruitment protein (Amer1, also known as WTX) represses WNT/ β -catenin signaling (Grohmann et al., 2007; Rivera et al., 2007; Tanneberger et al., 2011); it contains a strong BH signal but a weak aPKC phosphosite score (Figures 5C and 5H). Correspondingly, we found that the Amer1 PRBH is targeted

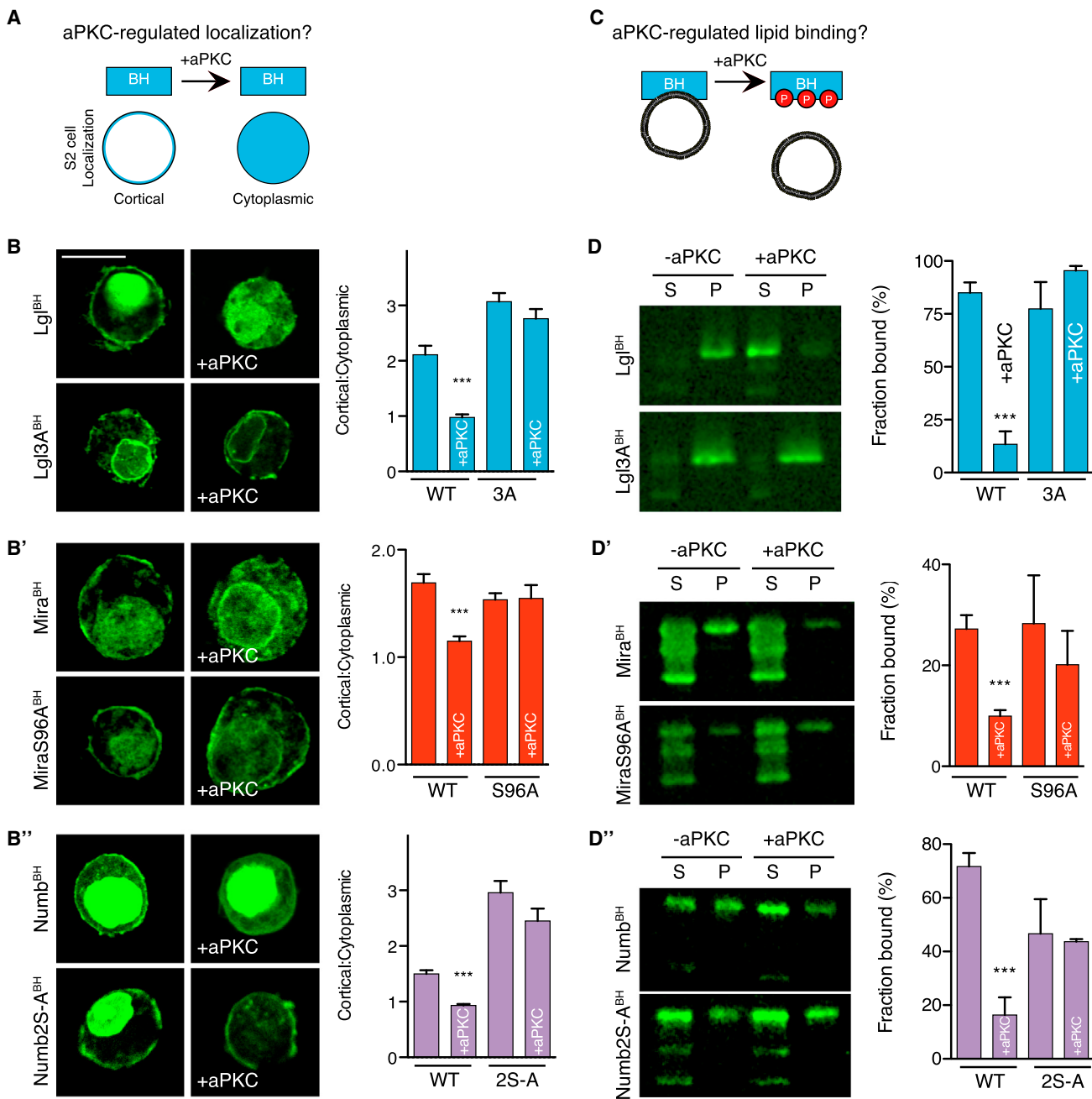


Figure 4. Phosphorylation Directly Inhibits Par Substrate BH Motif Interactions with Phospholipids and the Cell Cortex

(A) Schematic of aPKC regulation of BH motif cortical localization assay.

(B–B'') Phosphorylation by aPKC disrupts Lg^{BH} (B), Mira^{BH} (B'), and Numb^{BH} (B'') BH motif cortical enrichment. The localization of EGFP fused BH motifs both in the absence and presence (+aPKC) of aPKC is shown, along with that for BH motifs with phosphorylation sites mutated to alanine (3A, S96A, S48AS52A). Expression of aPKC was verified by immunostaining. Representative images from each transfection are shown. Expression of aPKC reduces cortical enrichment, and this reduction is dependent on the presence of the phosphorylation site. The mean and SEM are shown for measurements from at least 16 cells. Asterisks indicate $p < 0.0001$ as assessed by a non-parametric t test to compare each aPKC-expressing cell to its respective control without aPKC expression. Scale bar, 10 μ m. See also Figure S3A.

(C) The effect of aPKC phosphorylation on phospholipid binding was tested with lipid cosedimentation assays.

(D–D'') Effect of aPKC on Par substrate BH motif binding to PC/PS/PIP₂ vesicles. Lipid-binding cosedimentation assays were performed in the presence of aPKC and ATP. Samples were analyzed by immunoblotting for the MBP tag. S marks the supernatant and P marks the pellet. The “S-to-A” mutations are: Lg3A (D), MiraS96A (D'), and NumbS48AS52A (D''). All vesicles were composed of 4:1 PC:PS plus 10% PIP₂. The fraction of protein bound, quantified as the amount of protein in the pellet over total protein, was quantified in triplicate for each vesicle composition. The mean and SEM of the fraction bound are shown. * $p < 0.0001$. Significance was evaluated using a non-parametric t test relative to binding in the absence of aPKC. See also Figures S3.

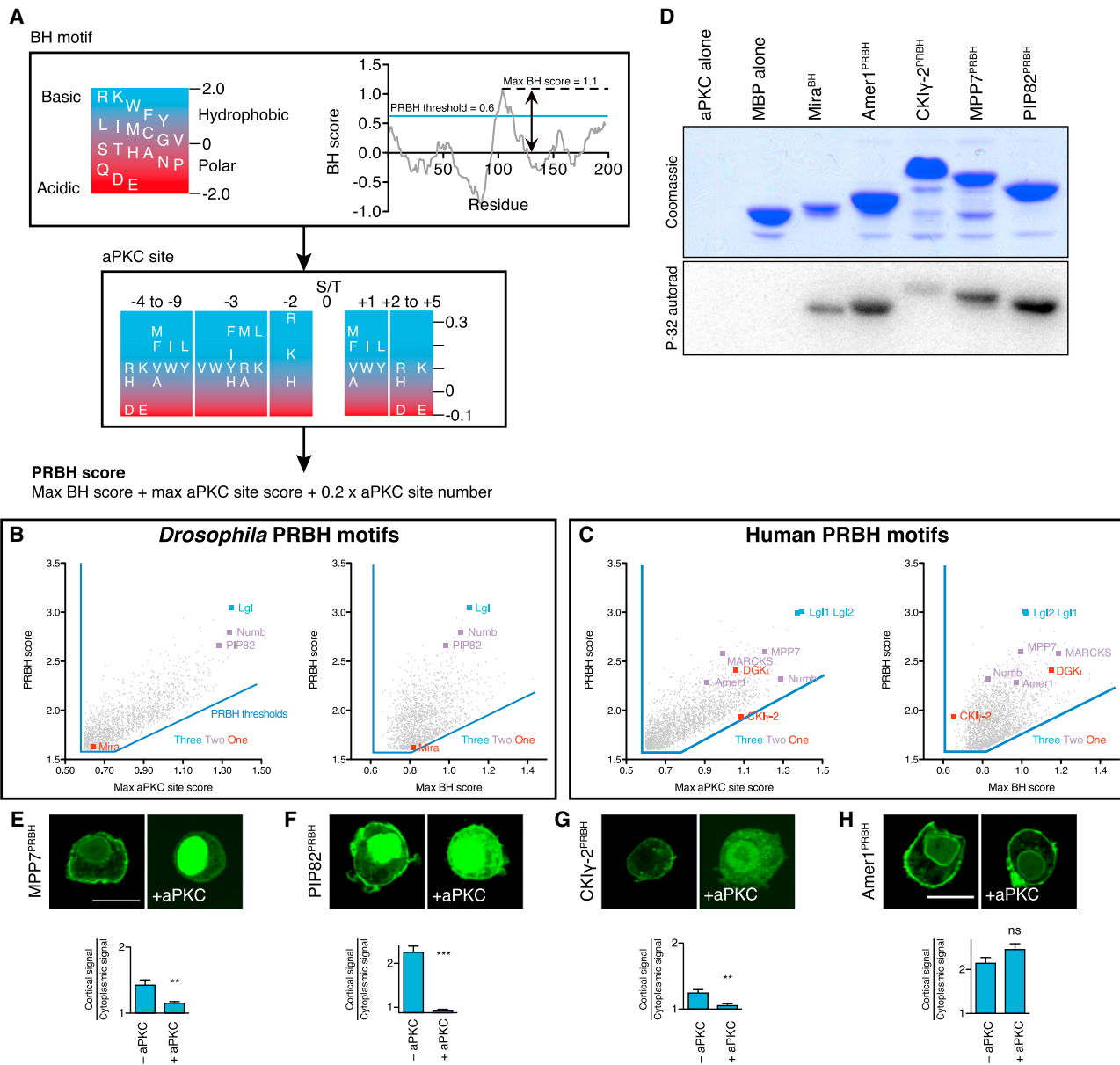


Figure 5. PRBHscreen Identifies Candidate aPKC-Regulated PRBH Motifs

(A) Schematic representation of bioinformatics identification of PRBH motifs from proteomic files. The BH motif scoring algorithm identifies sequences with strong BH character. Vertical position on a scale from -2 to 2 shows each residues' BH score. A representative BH plot has been included to depict the maximum BH score. aPKC consensus sites were identified and scored by scanning for S/T residues with preferred residues in the specific NH₂- and COOH-terminal sites. The scale shows the aPKC site score (ranging from -0.1 to 0.35) for each residue in the specified site. Unlisted residues have no effect on the overall phosphosite score. An overall PRBH score was assigned to sequences identified in both the BH and aPKC site identifying algorithm.

(B and C) PRBH score distribution from in the *Drosophila* and human proteome. Select PRBH motifs from the fly and human proteome are highlighted in (B) and (C), respectively. Gray points display each identified putative PRBH motif with its respective PRBH max BH score and max aPKC site score. Blue, purple and red denote the number of identified aPKC sites. Blue lines mark the PRBH threshold values, sequences with scores less than these values are not candidate PRBH motifs. See also Figure S4 and Table S1 for analysis of the *Caenorhabditis elegans* and sponge proteomes.

(D) aPKC phosphorylates candidate PRBH motifs. A ³²P autoradiograph demonstrates that Amer1^{PRBH}, CKIγ-2^{PRBH}, MPP7^{PRBH}, and PIP82^{PRBH} are phosphorylated by aPKC. A Coomassie-stained loading control gel is displayed.

(E-H) aPKC inhibits localization to the cell cortex for several candidate PRBH motifs. Representative images are shown with a quantification of the cortical to cytoplasmic signal intensity ratio as the mean ± SEM. Cartoons show the constructs characterized with candidate aPKC phosphosites listed. Each protein was characterized as an EGFP-fusion protein. Statistical significance testing was performed using the t test of aPKC cotransfected cells to singly transfected cells. **p < 0.001, ***p < 0.0001. Significance was evaluated using a non-parametric t test relative of the singly transfected cells to aPKC cotransfected cells. ns, not significant.

See also Figure S4.

to the cell cortex, but aPKC expression does not reduce its cortical localization (Figure 5H). However, the number of potential phospho-accepting residues within Amer1's PRBH makes it a prime candidate for regulation by another kinase. We conclude that the PRBH algorithm is a good predictor of aPKC-regulated cortical association, with higher scoring motifs more likely to exhibit this behavior. Furthermore, a more precise assessment of PRBH character can be made by directly comparing BH motif area, the number of aPKC phosphosites, etc.

DISCUSSION

The organization of the animal cell cortex by the Par complex involves two key steps (Goehring, 2014; Goldstein and Macara, 2007; Knoblich, 2010; Prehoda, 2009). The first involves the specification of the Par domain by upstream components such as the Rho GTPase Cdc42. In the second, diverse proteins must "plug into" Par polarity by occupying cortical areas that lack the Par complex. We have examined how the key output of the Par complex, aPKC activity, leads to cortical exclusion of the diverse array of Par-polarized proteins. Our approach was to examine the cortical interactions of three Par substrates that had no described sequence or domain similarities and to determine how aPKC phosphorylation modulates their cortical binding. Although these Par substrates do not have clear sequence homology, they each contain a "phospho-regulated BH" motif that couples aPKC phosphorylation to membrane affinity. This coupling is a direct consequence of the overlap of BH and aPKC phosphorylation sites in the PRBH motif as this allows phosphorylation to have a significant effect on the electrostatic character of the sequence. Using this defining feature, we developed a computational approach for identifying candidate PRBH motifs, which we validated that aPKC regulates cortical association of several hits from the human and fly proteomes. We expect this technique will be useful for identifying candidate polarity proteins and proteins involved in other cellular processes where regulated membrane association is important.

Multivalent Interactions Mediate Par Substrate Cortical Localization

We have found that Par substrate BH motifs localize to the cortex, but it is important to note that robust targeting requires elements outside of the BH sequence. While our data suggest that PRBH motifs are key regulatory elements for polarity, the requirement of additional interactions for high-affinity cortical interactions means that they are unlikely to lead to substrate polarity on their own. Similar "multivalent" interaction mechanisms has been observed with other BH motif-containing proteins that are regulated by phosphorylation and utilize accessory interactions to enhance their cortical targeting, including the yeast pheromone signaling protein Ste5 (Pryciak and Huntress, 1998; Winters et al., 2005) and the actin filament crosslinker MARCKS (Hartwig et al., 1992; McLaughlin and Murray, 2005; Thelen et al., 1991). In Ste5, protein-protein interactions provide additional cortex affinity, whereas MARCKS contains a myristoyl modification that works with its BH motif (George and Blackshear, 1992). The multivalent nature of protein-phospholipid interactions mediated by BH motifs may explain why protein-protein interactions are important to polarize some Par substrates. For

example, Lgl interacts with non-muscle myosin II (Betschinger et al., 2005), and this interaction may cooperate with BH-phospholipid binding to yield the increased cortical interaction of full-length Lgl compared to its BH alone. Phospholipid binding by the BH motif and the PTB domain may robustly target Numb to the cell cortex (Dho et al., 1999). However, in order for cortical localization to be regulated, the accessory interactions must not be stable enough to mediate cortical targeting on their own, or alternatively they must themselves be regulated by phosphorylation (McLaughlin and Murray, 2005; Strickfaden et al., 2007). Future studies of candidate PRBH-containing proteins will determine which regulated interactions are used for Par-mediate polarity and how factors such as cortical binding affinities, multiple PRBH motifs, and cortical mobility cooperate to mediate substrate polarization.

PRBH: A Mechanism for Convergent Evolution of Par-Mediated Polarity?

Phosphorylation can regulate protein activity by several means, including allostery and conformational changes (Cohen, 2000; Johnson and Barford, 1993; Serber and Ferrell, 2007). In this type of regulation, phosphate attachment to a specific side chain alters protein structural features and/or dynamics that are important for catalytic or binding activity (Barford et al., 1991). This coupling requires a connection between the phosphorylation site and the native state energy landscape, such that the phosphorylation site sequence is typically highly conserved (Holt et al., 2009). Allosteric effects or conformational changes may induce the polarization of substrates that lack PRBH motifs (e.g., Baz/Par-3 and Par-1) (Hurov et al., 2004; Morais-de-Sá et al., 2010; Sotillo et al., 2004; Suzuki et al., 2004). In contrast to complex mechanisms like these, phosphorylation of many Par substrates alters activity by changing the bulk electrostatics of the phospholipid binding sequence (Serber and Ferrell, 2007). Here, phosphorylation must occur close to the binding sequence but does not have to be coupled to structural or dynamic changes in the protein (Holt et al., 2009). Because many sequences satisfy the requirements of (1) an electrostatic character sufficient for binding negatively charged phospholipids, and (2) one or more aPKC phosphorylation sites, we propose that the sequence path for convergent evolution of PRBH motifs could be fairly simple. An existing motif, either BH or aPKC phosphosite is likely to require a small number of mutations to retain existing function while causing a gain of the missing function. For example, a protein that is advantageously targeted to the membrane via a BH motif could require only a small number of mutations to become polarized with the introduction of one or more aPKC phosphosites.

Functions of Candidate PRBH-Containing Proteins

We identified several proteins whose cortical localization is regulated by aPKC: MPP7 and PIP82 and CKI γ -2. In epithelial cells, MPP7 localizes to the lateral cortex and mediates tight junction formation (Stucke et al., 2007). While previous work has not implicated aPKC in its regulation, its localization and aPKC's inhibition of cortical localization make it a strong candidate Par-polarized substrate. The localization of several Casein kinase paralogs that lack predicted PRBH motifs (Table S1) have been described (Davidson et al., 2005; Gross et al.,

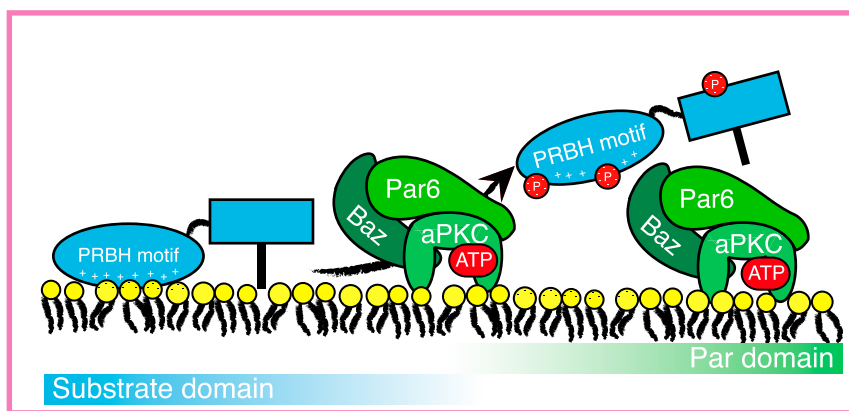


Figure 6. Model for Par Polarization by Phosphoregulated BH Motifs

PRBH motifs mediate localization to regions of the cell cortex opposite the Par complex. The box detail shows the molecular interactions occurring at the interface between the Par and substrate domains. Par substrates will localize to the cortex by electrostatic interactions with phospholipids until they encounter aPKC and become phosphorylated. Phosphorylation reduces their membrane affinity. Weak accessory interactions mediate localization to the cell cortex but they must allow the substrate to dissociate from the cell cortex, when the BH motif is phosphorylated.

1997), although the localization of the PRBH-containing CKI γ -2 in a polarized *in vivo* context is uncharacterized to our knowledge. However, recent work demonstrated that the CKI γ -associated protein Lrp6 localizes to the basolateral cortex in the neuroepithelium (Davidson et al., 2005; Huang and Niehrs, 2014), suggesting that CKI γ -2 may also exhibit this pattern of localization. Future work will need to address if aPKC indeed regulates CKI γ -2 localization *in vivo*. The localization and molecular function of PIP82 in *Drosophila* photoreceptor cells has not been described, but it is intriguing that light exposure causes it to be dephosphorylated (Suri et al., 1998). If the PIP82 PRBH is dephosphorylated during this process, it would be a mechanism for coupling cortical localization to light exposure. While we have identified many putative aPKC-regulated PRBH motifs, future work will need to address how this regulatory sequence is used cellular processes besides polarity. One particularly enticing PRBH protein is the retromer component Vps26 as it has been implicated in Par- and Scribble-mediated endosomal trafficking (de Vreede et al., 2014). Characterization of Vps26 and other PRBH proteins will likely emphasize the diverse functions of aPKC phosphorylation.

A Model for Protein Polarization Directed by the Par Complex

From these studies, we propose a model for Par complex function (Figure 6). In this model, Par-polarized substrates localize to the cortex via direct interactions between their BH motifs and membrane phospholipids. When a substrate enters the Par domain, either from the cytoplasm or by diffusion along the membrane, it becomes phosphorylated by aPKC. Addition of phosphates alters the electrostatics of the PRBH motif to reduce its affinity for phospholipids causing it to be displaced into the cytoplasm. Future work will be required to complete the “life cycle” of these substrates to understand the fate of Par substrates once displaced into the cytoplasm. Phosphorylation may be coupled to inactivation, degradation, or phosphatase-mediated re-association to the cortex.

EXPERIMENTAL PROCEDURES

Sequence Analysis and Computational Work

BH motifs were initially identified using BH-search: a computational algorithm described in Brzeska et al. (2010) and is available online (<http://helixweb.nih.gov/bhsearch/>).

Domain analyses were performed using SMART (Letunic et al., 2015; Schultz et al., 1998). Figures were assembled using the Adobe Creative Suite. The PRBH algorithm was implemented using the Python programming language with standard Python libraries including numpy and matplotlib. The *Drosophila* and human non-redundant proteome were analyzed from the EMBL-EBI reference proteome files. Please see the *Supplemental Information* for the full script and a detailed description of the PRBH identification program. Briefly, BH motifs were identified using a previously described BH scoring metric (Brzeska et al., 2010). Residues surrounding S/T residues were scored based on the aPKC consensus sequence (Wang et al., 2012) with Miranda’s aPKC recognition sequence included. Composite scores were assigned to sequences identified as BH motifs and aPKC consensus sequences. PRBH scores above a threshold value were analyzed.

Molecular Cloning and Cell Culture

All molecular cloning was performed as previously described (Graybill et al., 2012). Please see the *Supplemental Experimental Procedures* for details. Cell culture was performed as previously described (Lu and Prehoda, 2013). Briefly, cells were grown according to manufacturer’s protocol, transiently transfected with Effectene (QIAGEN). Transfected cells were fixed and immunostained as previously described (Lu and Prehoda, 2013) and imaged with the following confocal microscopes: Olympus Fluoview FV1000 BX61 with a PlanApo N 60 \times /1.42 oil and a Leica SP2 confocal microscope with a 63 \times /1.40–0.60 oil CS objective. All proteins were tagged at their NH₂ terminus. Image analysis was performed with ImageJ.

Protein Expression and Purification

Protein expression was performed as previously described (Graybill et al., 2012). Briefly, MBP-tagged proteins were purified from BL21 (DE3) cells by amylose affinity purification. aPKC was purified from HEK293F cells transiently transfected with 293fectin transfection reagent (Life Technology). All His₆-tagged aPKC constructs were purified with Ni²⁺-nitritriacetic acid resin purification from HEK293F cell lysates. Please see the *Supplemental Experimental Procedures* for a detailed description of this protein purification.

Biochemical Assays

All lipids were purchased from Avanti Polar Lipids. Giant unilamellar vesicles were prepared as previously described (Winters et al., 2005). Please see the *Supplemental Experimental Procedures* for details of on vesicle preparation and lipid cosedimentation assays. Pelleting assays were performed as previously described (Prehoda et al., 2000). Giant unilamellar vesicles and associated bound proteins were pelleted by ultracentrifugation and analyzed by SDS-PAGE. Kinase assays were performed as previously described (Atwood and Prehoda, 2009; Graybill et al., 2012). Briefly, aPKC and substrates were incubated in assay buffer (50 mM Tris-HCl, pH 7.5, 100 mM NaCl, 10 mM MgCl₂) at 30°C for 5 min before addition of 1 mM ATP doped with [γ -³²P] ATP (~1.0 \times 10⁵/nmol of ATP). The kinase reaction proceeded for 30 min before quenching with SDS loading dye. Samples were run on a 12.5%

acrylamide SDS-PAGE gel, then analyzed with the Storm 860 Molecular Imager and a phosphor screen (Molecular Dynamics).

SUPPLEMENTAL INFORMATION

Supplemental Information includes Supplemental Experimental Procedures, four figures, and one table and can be found with this article online at <http://dx.doi.org/10.1016/j.devcel.2015.09.016>.

AUTHOR CONTRIBUTIONS

All experiments were designed and conceived by M.J.B. and K.E.P. M.J.B. performed all experiments. Programming was performed by M.J.B. and K.E.P. The manuscript was written by M.J.B. and K.E.P.

ACKNOWLEDGMENTS

Plasmids were generously provided by Roland Le Borgne (Numb), Gabrielle Boulianne (Neuralized), Kentaro Hanada (CKI γ -2), and Jürgen Behrens (Amer1). Thanks to Robert Lyle McPherson for his assistance with cell culture and protein purification. We would like to thank Michael Drummond, Chiharu Graybill, Ryan Holly, Kimberly Jones, Robert Lyle McPherson, and Brett Wee for useful discussions, and J. Andy Berglund and Raghavendra Parthasarathy for equipment use. Thanks to Tom Stevens, Brad Nolen, and Chris Doe for comments on the manuscript and to Peter Pryciak for useful discussions about this work. This work was supported by the NIH Predoctoral Training grant GM007759 (M.J.B.) and NIH grant GM068032 (K.E.P.).

Received: April 29, 2015

Revised: September 3, 2015

Accepted: September 23, 2015

Published: October 15, 2015

REFERENCES

- Atwood, S.X., and Prehoda, K.E. (2009). aPKC phosphorylates Miranda to polarize fate determinants during neuroblast asymmetric cell division. *Curr. Biol.* 19, 723–729.
- Barford, D., Hu, S.H., and Johnson, L.N. (1991). Structural mechanism for glycogen phosphorylase control by phosphorylation and AMP. *J. Mol. Biol.* 218, 233–260.
- Betschinger, J., Mechtler, K., and Knoblich, J.A. (2003). The Par complex directs asymmetric cell division by phosphorylating the cytoskeletal protein Lgl. *Nature* 422, 326–330.
- Betschinger, J., Eisenhaber, F., and Knoblich, J.A. (2005). Phosphorylation-induced autoinhibition regulates the cytoskeletal protein Lethal (2) giant larvae. *Curr. Biol.* 15, 276–282.
- Brzeska, H., Guag, J., Remmert, K., Chacko, S., and Korn, E.D. (2010). An experimentally based computer search identifies unstructured membrane-binding sites in proteins: application to class I myosins, PAKS, and CARMIL. *J. Biol. Chem.* 285, 5738–5747.
- Cline, E.G., and Nelson, W.J. (2007). Characterization of mammalian Par 6 as a dual-location protein. *Mol. Cell. Biol.* 27, 4431–4443.
- Cohen, P. (2000). The regulation of protein function by multisite phosphorylation—a 25 year update. *Trends Biochem. Sci.* 25, 596–601.
- Cuenca, A.A., Schetter, A., Aceto, D., Kemphues, K., and Seydoux, G. (2003). Polarization of the *C. elegans* zygote proceeds via distinct establishment and maintenance phases. *Development* 130, 1255–1265.
- Davidson, G., Wu, W., Shen, J., Bilic, J., Fenger, U., Stannek, P., Glinka, A., and Niehrs, C. (2005). Casein kinase 1 gamma couples Wnt receptor activation to cytoplasmic signal transduction. *Nature* 438, 867–872.
- de Vreede, G., Schoenfeld, J.D., Windler, S.L., Morrison, H., Lu, H., and Bilder, D. (2014). The Scribble module regulates retromer-dependent endocytic trafficking during epithelial polarization. *Development* 141, 2796–2802.
- Dho, S.E., French, M.B., Woods, S.A., and McGlade, C.J. (1999). Characterization of four mammalian numb protein isoforms. Identification of cytoplasmic and membrane-associated variants of the phosphotyrosine binding domain. *J. Biol. Chem.* 274, 33097–33104.
- Dho, S.E., Trejo, J., Siderovski, D.P., and McGlade, C.J. (2006). Dynamic regulation of mammalian numb by G protein-coupled receptors and protein kinase C activation: Structural determinants of numb association with the cortical membrane. *Mol. Biol. Cell* 17, 4142–4155.
- Engelman, D.M. (2005). Membranes are more mosaic than fluid. *Nature* 438, 578–580.
- Farese, R.V., Lee, M.C., and Sajan, M.P. (2014). Atypical PKC: a target for treating insulin-resistant disorders of obesity, the metabolic syndrome and type 2 diabetes mellitus. *Expert Opin. Ther. Targets* 18, 1163–1175.
- Fuerstenberg, S., Peng, C.Y., Alvarez-Ortiz, P., Hor, T., and Doe, C.Q. (1998). Identification of Miranda protein domains regulating asymmetric cortical localization, cargo binding, and cortical release. *Mol. Cell. Neurosci.* 12, 325–339.
- George, D.J., and Blackshear, P.J. (1992). Membrane association of the myristoylated alanine-rich C kinase substrate (MARCKS) protein appears to involve myristate-dependent binding in the absence of a myristoyl protein receptor. *J. Biol. Chem.* 267, 24879–24885.
- Goehring, N.W. (2014). PAR polarity: from complexity to design principles. *Exp. Cell Res.* 328, 258–266.
- Goldstein, B., and Macara, I.G. (2007). The PAR proteins: fundamental players in animal cell polarization. *Dev. Cell* 13, 609–622.
- Graybill, C., and Prehoda, K.E. (2014). Ordered multisite phosphorylation of lethal giant larvae by atypical protein kinase C. *Biochemistry* 53, 4931–4937.
- Graybill, C., Wee, B., Atwood, S.X., and Prehoda, K.E. (2012). Partitioning-defective protein 6 (Par-6) activates atypical protein kinase C (aPKC) by pseudosubstrate displacement. *J. Biol. Chem.* 287, 21003–21011.
- Grohmann, A., Tanneberger, K., Alzner, A., Schneikert, J., and Behrens, J. (2007). AMER1 regulates the distribution of the tumor suppressor APC between microtubules and the plasma membrane. *J. Cell Sci.* 120, 3738–3747.
- Gross, S.D., Simerly, C., Schatten, G., and Anderson, R.A. (1997). A casein kinase I isoform is required for proper cell cycle progression in the fertilized mouse oocyte. *J. Cell Sci.* 110, 3083–3090.
- Groves, J.T., and Kuriyan, J. (2010). Molecular mechanisms in signal transduction at the membrane. *Nat. Struct. Mol. Biol.* 17, 659–665.
- Hao, Y., Boyd, L., and Seydoux, G. (2006). Stabilization of cell polarity by the *C. elegans* RING protein PAR-2. *Dev. Cell* 10, 199–208.
- Harris, T.J.C., and Peifer, M. (2005). The positioning and segregation of apical cues during epithelial polarity establishment in *Drosophila*. *J. Cell Biol.* 170, 813–823.
- Hartwig, J.H., Thelen, M., Rosen, A., Janmey, P.A., Nairn, A.C., and Aderem, A. (1992). MARCKS is an actin filament crosslinking protein regulated by protein kinase C and calcium-calmodulin. *Nature* 356, 618–622.
- Holt, L.J., Tuch, B.B., Villén, J., Johnson, A.D., Gygi, S.P., and Morgan, D.O. (2009). Global analysis of Cdk1 substrate phosphorylation sites provides insights into evolution. *Science* 325, 1682–1686.
- Huang, Y.-L., and Niehrs, C. (2014). Polarized Wnt signaling regulates ectodermal cell fate in *Xenopus*. *Dev. Cell* 29, 250–257.
- Hurov, J.B., Watkins, J.L., and Piwnica-Worms, H. (2004). Atypical PKC phosphorylates PAR-1 kinases to regulate localization and activity. *Curr. Biol.* 14, 736–741.
- Johnson, L.N., and Barford, D. (1993). The effects of phosphorylation on the structure and function of proteins. *Annu. Rev. Biophys. Biomol. Struct.* 22, 199–232.
- Knoblich, J.A. (2010). Asymmetric cell division: recent developments and their implications for tumour biology. *Nat. Rev. Mol. Cell Biol.* 11, 849–860.
- Knoblich, J.A., Jan, L.Y., and Jan, Y.N. (1997). The N terminus of the *Drosophila* Numb protein directs membrane association and actin-dependent asymmetric localization. *Proc. Natl. Acad. Sci. USA* 94, 13005–13010.
- Lemmon, M.A. (2008). Membrane recognition by phospholipid-binding domains. *Nat. Rev. Mol. Cell Biol.* 9, 99–111.

- Letunic, I., Doerks, T., and Bork, P. (2015). SMART: recent updates, new developments and status in 2015. *Nucleic Acids Res.* 43, D257–D260.
- Lu, M.S., and Prehoda, K.E. (2013). A NudE/14-3-3 pathway coordinates dynein and the kinesin Khc73 to position the mitotic spindle. *Dev. Cell* 26, 369–380.
- Luo, B., Prescott, S.M., and Topham, M.K. (2003). Protein kinase C alpha phosphorylates and negatively regulates diacylglycerol kinase zeta. *J. Biol. Chem.* 278, 39542–39547.
- Martin-Belmonte, F., Gassama, A., Datta, A., Yu, W., Rescher, U., Gerke, V., and Mostov, K. (2007). PTEN-mediated apical segregation of phosphoinositides controls epithelial morphogenesis through Cdc42. *Cell* 128, 383–397.
- Matsuzaki, F., Ohshiro, T., Ikeshima-Kataoka, H., and Izumi, H. (1998). miranda localizes staufen and prospero asymmetrically in mitotic neuroblasts and epithelial cells in early *Drosophila* embryogenesis. *Development* 125, 4089–4098.
- McLaughlin, S. (1989). The electrostatic properties of membranes. *Annu. Rev. Biophys. Biophys. Chem.* 18, 113–136.
- McLaughlin, S., and Murray, D. (2005). Plasma membrane phosphoinositide organization by protein electrostatics. *Nature* 438, 605–611.
- Morais-de-Sá, E., Mirouse, V., and St Johnston, D. (2010). aPKC phosphorylation of Bazooka defines the apical/lateral border in *Drosophila* epithelial cells. *Cell* 141, 509–523.
- Morone, N., Fujiwara, T., Murase, K., Kasai, R.S., Ike, H., Yuasa, S., Usukura, J., and Kusumi, A. (2006). Three-dimensional reconstruction of the membrane skeleton at the plasma membrane interface by electron tomography. *J. Cell Biol.* 174, 851–862.
- Overeem, A.W., Bryant, D.M., and van IJzendoorn, S.C.D. (2015). Mechanisms of apical-basal axis orientation and epithelial lumen positioning. *Trends Cell Biol.* 25, 476–485.
- Papayannopoulos, V., Co, C., Prehoda, K.E., Snapper, S., Taunton, J., and Lim, W.A. (2005). A polybasic motif allows N-WASP to act as a sensor of PIP(2) density. *Mol. Cell* 17, 181–191.
- Prehoda, K.E. (2009). Polarization of *Drosophila* neuroblasts during asymmetric division. *Cold Spring Harb. Perspect. Biol.* 1, a001388.
- Prehoda, K.E., Scott, J.A., Mullins, R.D., and Lim, W.A. (2000). Integration of multiple signals through cooperative regulation of the N-WASP-Arp2/3 complex. *Science* 290, 801–806.
- Pryciak, P.M., and Huntress, F.A. (1998). Membrane recruitment of the kinase cascade scaffold protein Ste5 by the Gbetagamma complex underlies activation of the yeast pheromone response pathway. *Genes Dev.* 12, 2684–2697.
- Rivera, M.N., Kim, W.J., Wells, J., Driscoll, D.R., Brannigan, B.W., Han, M., Kim, J.C., Feinberg, A.P., Gerald, W.L., Vargas, S.O., et al. (2007). An X chromosome gene, WTX, is commonly inactivated in Wilms tumor. *Science* 315, 642–645.
- Rohatgi, R., Ma, L., Miki, H., Lopez, M., Kirchhausen, T., Takenawa, T., and Kirschner, M.W. (1999). The interaction between N-WASP and the Arp2/3 complex links Cdc42-dependent signals to actin assembly. *Cell* 97, 221–231.
- Rolls, M.M., Albertson, R., Shih, H.-P., Lee, C.-Y., and Doe, C.Q. (2003). *Drosophila* aPKC regulates cell polarity and cell proliferation in neuroblasts and epithelia. *J. Cell Biol.* 163, 1089–1098.
- Schober, M., Schaefer, M., and Knoblich, J.A. (1999). Bazooka recruits Inscuteable to orient asymmetric cell divisions in *Drosophila* neuroblasts. *Nature* 402, 548–551.
- Schultz, J., Milpetz, F., Bork, P., and Ponting, C.P. (1998). SMART, a simple modular architecture research tool: identification of signaling domains. *Proc. Natl. Acad. Sci. USA* 95, 5857–5864.
- Serber, Z., and Ferrell, J.E., Jr. (2007). Tuning bulk electrostatics to regulate protein function. *Cell* 128, 441–444.
- Skwarek, L.C., Garroni, M.K., Commissio, C., and Boulian, G.L. (2007). Neuralized contains a phosphoinositide-binding motif required downstream of ubiquitination for delta endocytosis and notch signaling. *Dev. Cell* 13, 783–795.
- Smith, C.A., Lau, K.M., Rahmani, Z., Dho, S.E., Brothers, G., She, Y.M., Berry, D.M., Bonneil, E., Thibault, P., Schweigert, F., et al. (2007). aPKC-mediated phosphorylation regulates asymmetric membrane localization of the cell fate determinant Numb. *EMBO J.* 26, 468–480.
- Sotillos, S., Diaz-Meco, M.T., Caminero, E., Moscat, J., and Campuzano, S. (2004). DaPKC-dependent phosphorylation of Crumbs is required for epithelial cell polarity in *Drosophila*. *J. Cell Biol.* 166, 549–557.
- Standaert, M.L., Bandyopadhyay, G., Kanoh, Y., Sajan, M.P., and Farese, R.V. (2001). Insulin and PIP3 activate PKC-zeta by mechanisms that are both dependent and independent of phosphorylation of activation loop (T410) and autophosphorylation (T560) sites. *Biochemistry* 40, 249–255.
- Strand, D., Jakobs, R., Merdes, G., Neumann, B., Kalmes, A., Heid, H.W., Husmann, I., and Mechler, B.M. (1994). The *Drosophila* lethal(2)giant larvae tumor suppressor protein forms homo-oligomers and is associated with non-muscle myosin II heavy chain. *J. Cell Biol.* 127, 1361–1373.
- Strickfaden, S.C., Winters, M.J., Ben-Ari, G., Lamson, R.E., Tyers, M., and Pryciak, P.M. (2007). A mechanism for cell-cycle regulation of MAP kinase signaling in a yeast differentiation pathway. *Cell* 128, 519–531.
- Stucke, V.M., Timmerman, E., Vandekerckhove, J., Gevaert, K., and Hall, A. (2007). The MAGUK protein MPP7 binds to the polarity protein hDlg1 and facilitates epithelial tight junction formation. *Mol. Biol. Cell* 18, 1744–1755.
- Suri, V., Qian, Z., Hall, J.C., and Rosbash, M. (1998). Evidence that the TIM light response is relevant to light-induced phase shifts in *Drosophila melanogaster*. *Neuron* 21, 225–234.
- Suzuki, A., Yamanaka, T., Hirose, T., Manabe, N., Mizuno, K., Shimizu, M., Akimoto, K., Izumi, Y., Ohnishi, T., and Ohno, S. (2001). Atypical protein kinase C is involved in the evolutionarily conserved par protein complex and plays a critical role in establishing epithelia-specific junctional structures. *J. Cell Biol.* 152, 1183–1196.
- Suzuki, A., Hirata, M., Kamimura, K., Maniwa, R., Yamanaka, T., Mizuno, K., Kishikawa, M., Hirose, H., Amano, Y., Izumi, N., et al. (2004). aPKC acts upstream of PAR-1b in both the establishment and maintenance of mammalian epithelial polarity. *Curr. Biol.* 14, 1425–1435.
- Swierczynski, S.L., and Blackshear, P.J. (1996). Myristylation-dependent and electrostatic interactions exert independent effects on the membrane association of the myristylated alanine-rich protein kinase C substrate protein in intact cells. *J. Biol. Chem.* 271, 23424–23430.
- Tanneberger, K., Pfister, A.S., Brauburger, K., Schneiker, J., Hadjihannas, M.V., Kriz, V., Schulte, G., Bryja, V., and Behrens, J. (2011). Amer1/WTX couples Wnt-induced formation of PtdIns(4,5)P2 to LRP6 phosphorylation. *EMBO J.* 30, 1433–1443.
- Tepass, U. (2012). The apical polarity protein network in *Drosophila* epithelial cells: regulation of polarity, junctions, morphogenesis, cell growth, and survival. *Annu. Rev. Cell Dev. Biol.* 28, 655–685.
- Thelen, M., Rosen, A., Nairn, A.C., and Aderem, A. (1991). Regulation by phosphorylation of reversible association of a myristylated protein kinase C substrate with the plasma membrane. *Nature* 351, 320–322.
- Tomishige, N., Kumagai, K., Kusuda, J., Nishijima, M., and Hanada, K. (2009). Casein kinase Igamma2 down-regulates trafficking of ceramide in the synthesis of sphingomyelin. *Mol. Biol. Cell* 20, 348–357.
- Topham, M.K., Bunting, M., Zimmerman, G.A., McIntyre, T.M., Blackshear, P.J., and Prescott, S.M. (1998). Protein kinase C regulates the nuclear localization of diacylglycerol kinase-zeta. *Nature* 394, 697–700.
- Überall, F., Giselbrecht, S., Hellbert, K., Fresser, F., Bauer, B., Gschwendt, M., Grunz, H.H., and Baier, G. (1997). Conventional PKC- α , novel PKC- ϵ and PKC- θ , but not atypical PKC- λ are MARCKS kinases in intact NIH 3T3 fibroblasts. *J. Biol. Chem.* 272, 4072–4078.
- van Rossum, G. (2001). The Python Programming Language (Python Software Foundation).
- von Stein, W., Ramrath, A., Grimm, A., Müller-Borg, M., and Wodarz, A. (2005). Direct association of Bazooka/PAR-3 with the lipid phosphatase PTEN reveals a link between the PAR/aPKC complex and phosphoinositide signaling. *Development* 132, 1675–1686.

- Wang, C., Shang, Y., Yu, J., and Zhang, M. (2012). Substrate recognition mechanism of atypical protein kinase Cs revealed by the structure of PKC ζ in complex with a substrate peptide from Par-3. *Structure* 20, 791–801.
- Winters, M.J., Lamson, R.E., Nakanishi, H., Neiman, A.M., and Pryciak, P.M. (2005). A membrane binding domain in the ste5 scaffold synergizes with gbetagamma binding to control localization and signaling in pheromone response. *Mol. Cell* 20, 21–32.
- Wirtz-Peitz, F., Nishimura, T., and Knoblich, J.A. (2008). Linking cell cycle to asymmetric division: Aurora-A phosphorylates the Par complex to regulate Numb localization. *Cell* 135, 161–173.
- Wodarz, A., Ramrath, A., Kuchinke, U., and Knust, E. (1999). Bazooka provides an apical cue for Inscuteable localization in Drosophila neuroblasts. *Nature* 402, 544–547.
- Zhang, H., and Macara, I.G. (2006). The polarity protein PAR-3 and TIAM1 cooperate in dendritic spine morphogenesis. *Nat. Cell Biol.* 8, 227–237.
- Zhang, L., Wu, S.L., and Rubin, C.S. (2001). A novel adapter protein employs a phosphotyrosine binding domain and exceptionally basic N-terminal domains to capture and localize an atypical protein kinase C: characterization of *Caenorhabditis elegans* C kinase adapter 1, a protein that avidly binds protein kinase C3. *J. Biol. Chem.* 276, 10463–10475.

Developmental Cell

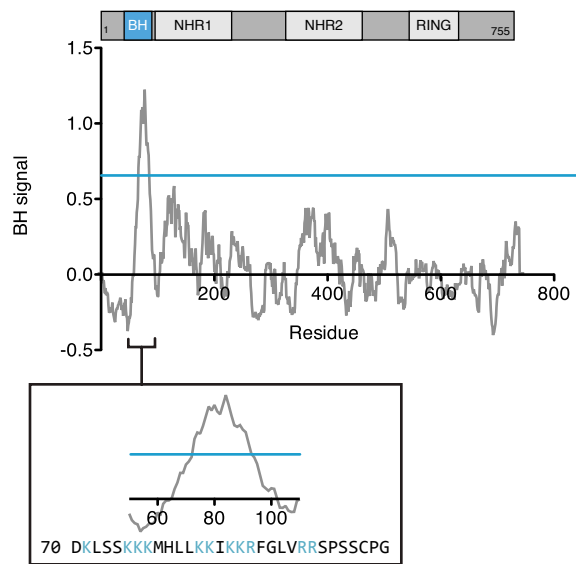
Supplemental Information

Establishment of Par-Polarized Cortical Domains

via Phosphoregulated Membrane Motifs

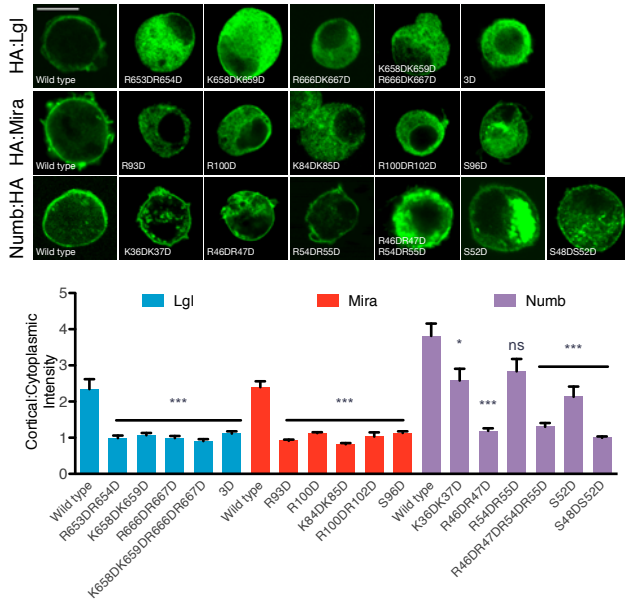
Matthew J. Bailey and Kenneth E. Prehoda

Supplemental Figure 1

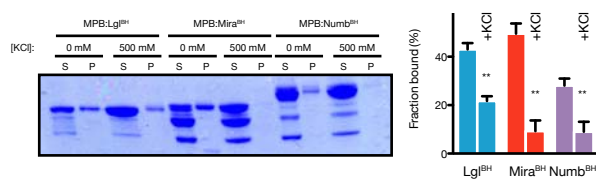


Supplemental Figure 2

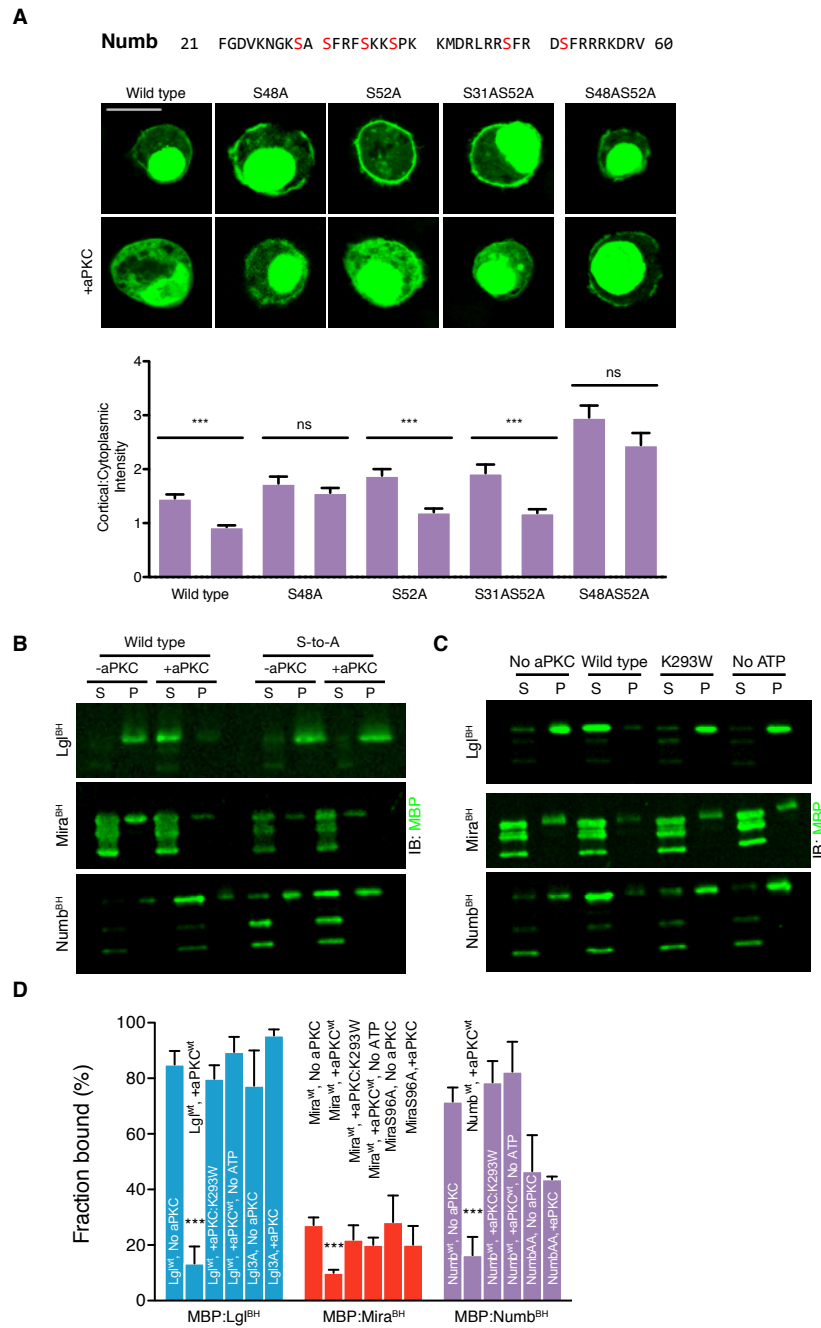
A



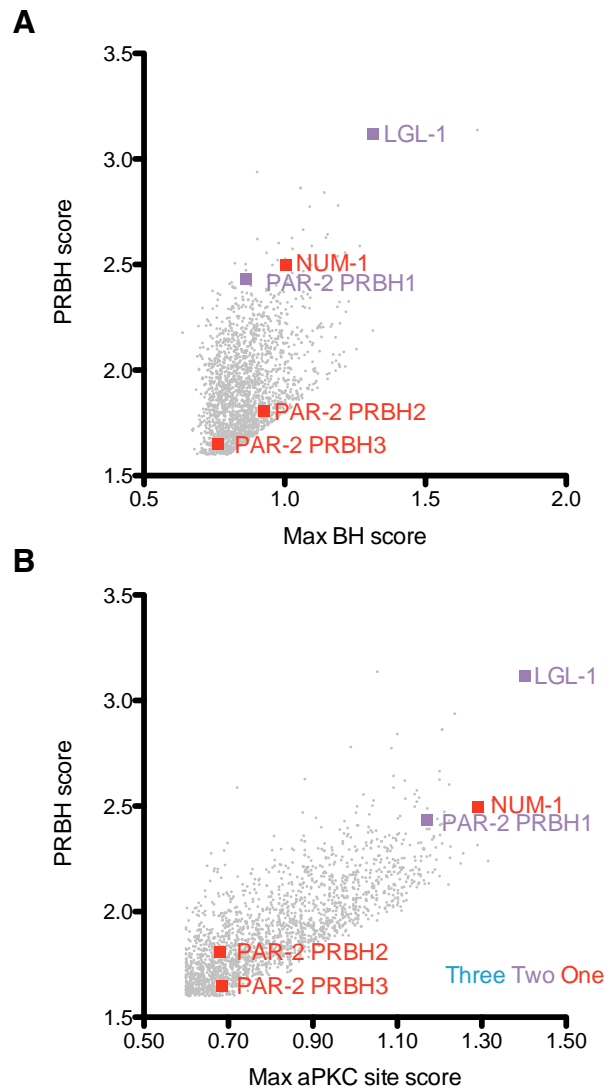
B



Supplemental Figure 3



Supplemental Figure 4



Supplemental Figure Legends

Supplemental Figure 1. Basic-Hydrophobic motif signal of Neur. Related to Figure 2.

The BH signal of Neur is plotted aligned to its domain architecture. The inset is a detail of Neur BH with basic residues colored blue. S residues within this region do not fit the aPKC consensus sequence which features a R in the -2 position and a hydrophobic residue in the +1 position, which makes it unlikely to be an aPKC-regulated PRBH motif. (Please see lower for further discussion of this). Abbreviations as follows: NHR, Neur homology region; RING, C₃HC₄ ring zinc finger.

Supplemental Figure 2. Charge mediates cortical targeting and phospholipid binding for Lgl, Mira, and Numb. Related to Figure 3.

A. Mutations to acidic residues reduce cortical localization of full length Lgl, Mira, and Numb. This Figure is related to Figure 3D but includes a larger set of point mutants. The localization of each full-length protein with point mutations was characterized by immunostaining transiently transfected S2 cells for the HA epitope tag. Localization was quantified as a cortical to cytoplasmic signal intensity ratio for at least 16 cells (mean ± SEM). Statistical testing was performed with t-test to compare the localization of each mutant to the wild type full-length control. A P-value of <0.05 and <0.0001 are marked with one and three asterisks, respectively. No statically significant difference is marked with ns. Scale bar, 10 μm.

B. High ionic strength disrupts BH phospholipid interactions. A Coomassie-stained gel from lipid vesicle-binding cosedimentation assays of vesicles with 4:1 PC:PS plus 10% PIP₂ is shown. Each BH motif was characterized as an MPB-fusion protein. The fraction of protein bound, quantified as the amount of protein in the pellet over total protein, was quantified in triplicate for each vesicle composition. The mean and SEM of the fraction bound are shown. Asterisks indicate p < 0.01. Significance was evaluated using a non-parametric t-test relative to low ionic strength.

Supplemental Figure 3. aPKC phosphorylation inhibits BH motif lipid binding for Lgl, Mira, and Numb. Related to Figure 4.

A. Identification of Numb BH residues involved in regulating aPKC-induced cortical

displacement. This figure is related to Figure 4B”, but includes a larger collection of Numb S-to-A mutations. The sequence of Numb BH is displayed with potential phosphorylation sites highlighted in red. Representative images from transiently transfected S2 cells in the absence or presence of aPKC are displayed. Cells were transfected with EGFP-tagged BH motifs. aPKC expression was verified by immunostaining for PKC ζ . The cortical to cytoplasmic intensity ratio was quantified and displayed as the mean \pm SEM, and statistical significance was determined by a non-parametric t-test to compare each mutant to its singly transfected control. P values of <0.0001 are marked with three asterisks. No statistical difference is marked by ns. Scale bar, 10 μ m.

B-D. aPKC kinase activity inhibits BH motif phospholipid binding. Images of representative immunoblots to characterize the effect of aPKC on Par substrate BH motif binding to PC/PS/PIP₂ vesicles are presented. Lipid-binding cosedimentation assays were performed in the presence of aPKC and ATP. For C, sample conditions varied as follows: No aPKC, ATP only; wild type, aPKC²⁵⁹⁻⁶⁰⁶ and ATP; K293W, aPKC K293W²⁵⁹⁻⁶⁰⁶ and ATP; No ATP, aPKC²⁵⁹⁻⁶⁰⁶ but no ATP. All samples contained 4:1 PC:PS plus 10% PIP₂ and all BH motifs had the wild type sequence. Samples were analyzed by immunoblotting for the MBP tag. S marks the supernatant and P marks the pellet. The “S-to-A” mutations are: Lgl3A, MiraS96A and NumbS48AS52A. Quantification of aPKC’s effect on BH motif vesicle binding displayed in A-B. The fraction of protein bound, quantified as the amount of protein in the pellet over total protein, was quantified in triplicate for each vesicle composition. The mean and SEM of the fraction bound are shown. Asterisks indicate p < 0.0001. Significance was evaluated using a non-parametric t-test relative to binding in the absence of aPKC.

Supplemental Figure 4. Distribution of PRBH scores in the *C. elegans* proteome.

Related to Figure 5.

A-B. PRBH scores, maximum BH score, and the highest aPKC site score are displayed from *C. elegans* proteome. Each point marks a single putative PRBH motif and all identified PRBH motifs are displayed. Blue lines mark the PRBH threshold values. Sequences with scores less than these values are not candidate PRBH motifs. See also Supplemental Data Table 1.

Extended Experimental Procedures

Sequence IDs and Residue Numbers

The following sequences were characterized in this study:

Lethal giant larvae: Species, *Drosophila melanogaster*; Symbol, Lethal (2) giant larvae; FlyBase ID, FBgn0002121; Isoform, PA (length 1161 residues). Lgl BH motif constructs include residues 647-681. Lgl ΔBH motif constructs deletes residues 647-681.

Miranda: Species, *Drosophila melanogaster*; Symbol, Mira; FlyBase ID, FBgn0021776; Isoform, PA (length 829 residues). Mira BH constructs include residues 71-110 and the BH motif deletion construct removes residues 72-110.

Numb: Species, *Drosophila melanogaster*; FlyBase ID, FBgn0002973; Isoform, PA (length 556 residues). Numb BH constructs include residues 15-86 and the BH motif deletion construct removes residues 24-56.

Neuralized: Species, *Drosophila melanogaster*; Symbol, Neur; Flybase ID, FBgn0002932; Isoform, PA (length 754 residues); BH motif, residues 68-88.

Amer1: Species, *Homo sapiens*; NCBI reference sequence, NP_689637.3; PRBH, residues 154-199.

Casein Kinase I gamma 2: Species, *Homo sapiens*; Symbol, CKIγ-2; NCBI reference sequence, GenBank ID, AAB88627.1. PRBH motif, 369-415.

MAGUK p55 subfamily member 7: Species, *Homo sapiens*; Symbol, MPP7; NCBI Reference Sequence, NP_775767.2. PRBH, residues 289-383.

PIP82: Species, *Drosophila melanogaster*; FlyBase ID, FGgn0024943. PRBH motif, residues 400-450.

Molecular cloning

All molecular cloning was performed as previously described (Graybill et al., 2012). MBP-fusion proteins were made using pMal C2 vector (New England BioLabs). The pMT v5-HisA with a HA-tag or pTub (Lu and Prehoda, 2013) promoter was used for S2 cell transient expression. All proteins were tagged with EGFP, MBP, or the HA epitope tag at the NH₂-terminus except for full-length Numb, which was COOH-terminally tagged. The Supplemental Experimental Procedures includes sequence IDs and residue numbers. The fragments of human MPP7 and fly PIP82 were cloned from synthetic gBlocks (IDT).

Cell culture and localization assays

Cell culture was performed as previously described (Lu and Prehoda, 2013). S2 cells were grown at 30°C in Schneider's media (Sigma-Aldrich) with 10% fetal bovine serum. S2 cells were transiently transfected with Effectene (QIAGEN) according to the manufacturer's protocol. Cells were seeded at $\sim 2 \times 10^6$ cells/well in a 6-well plate and transfected 24 hours later with 0.5 μ g plasmid. 24 hours after transfection, protein expression was induced for all pMT-transfected cells by addition of 0.5 mM CuSO₄. 24 hours post-induction, or 48 hours post-transfection for cells transfected with pTub plasmids, cells were plated on 12 mm glass coverslips in a 24-well plate for immunostaining and imaging.

For immunohistochemistry, cells were washed with PBS, and then fixed with 4% paraformaldehyde in PBS. Cells were washed with PBS with 0.1% saponin, washed three times with block [PBS, 0.1% saponin, and 1% bovine serum albumin (BSA)], and then blocked for 30 minutes with block. Primary antibody incubations were performed for either 1-2 hours at room temperature or overnight at 4°C. Cells were washed three times after immunostaining and between antibody staining steps. The following antibody dilutions were used: mouse anti-HA 1:1000 (Covance), rabbit anti-PKC ζ 1:1000 (Santa Cruz Biotechnology), DyLight 488 Donkey anti-mouse 1:500 (Jackson Immunoresearch) and DyLight Donkey 649 anti-rabbit (Jackson Immunoresearch). The cell cortex was stained with Alexa Fluor 555-Phalloidin (1:500, Invitrogen). Coverslips were mounted using Vectashield Hardset Mounting Medium (Vector Laboratories). An Olympus Fluoview FV1000 BX61 with a PlanApo N 60x/1.42 oil and a Leica SP2 confocal microscope with a 63x/1.40-0.60 oil CS objective was used to acquire all images. The cortical-to-cytoplasmic intensities were quantified in ImageJ using the free-hand line tool and freehand selection tool to determine the average fluorescence intensities in each cellular area. Prism was used for statistical analysis of quantified localization data. Images were processed with ImageJ and the Adobe Suite.

Protein expression and purification

MBP-fusion proteins were expressed and purified from BL21 (DE3) cells, as previously described (Graybill et al., 2012). Cells were lysed by sonication, pelleted by centrifugation at 15,000 rpm, 30 min, 4°C in a JA-20 rotor and the soluble fraction was bound to amylose resin (New England BioLabs) for 45 min, 4°C. The resin was washed

with MBP lysis buffer (20 mM Tris-HCl, pH 7.5, 200 mM NaCl, 1 mM EDTA, 1 mM DTT), then eluted with MBP elution buffer (20 mM Tris-HCl, pH 7.5, 200 mM NaCl, 1 mM EDTA, 1 mM DTT, 5 mM maltose). Elutions were pooled for dialysis in storage buffer (20 mM HEPES, pH 7.5, 50 mM NaCl, 1 mM DTT) overnight at 4°C and concentrated with a 10 kDa molecular weight cut-off Vivaspin 20 concentrator (GE Healthcare). Purified proteins were frozen with liquid nitrogen and stored at -80°C.

All His₆:aPKC²⁵⁹⁻⁶⁰⁶ (kinase domain) constructs were expressed in HEK293F cells by transient transfection using 293fectin transfection reagent (Life Technology). Transfections were performed according to manufacturer's protocols. Expressions and protein purification of aPKC was performed as previously described (Graybill et al., 2012). Briefly, cells were cultured at 37°C, 8% CO₂, 125 rpm in Freestyle HEK293-F media (Invitrogen). Cells were cotransfected with pCMV His₆-aPKC²⁵⁹⁻⁶⁰⁶ (wild type or K293W mutant) and pCMV GST:PDK1¹⁶¹⁻⁵⁰⁰ (kinase domain) at ~1.0×10⁶ cells/mL. Cells were harvested 24 hours post-transfection by centrifugation, resuspended in Ni²⁺ lysis buffer (50 mM NaH₃PO₄, 300 mM NaCl, 10 mM imidazole, pH adjusted to 8.0 with NaOH), then stored at -80°C. Cells were lysed by sonication, then lysates were pelleted by centrifugation at 15,000 rps, 30 min, 4°C in a JA-20 rotor. The supernatant was incubated with ammonium sulfate at a concentration of 45% (w/v) for 30 min, 4°C. Then, the solution was centrifuged at 15,000 rpm, 30 min, 4°C in a JA-20 rotor, the pellet was collected and resuspended in Ni²⁺ lysis buffer, then it was incubated with Ni²⁺-nitrilotriacetic acid resin (Qiagen) for 45 min, 4°C. Resin were washed with Ni²⁺ lysis buffer, then protein was eluted with Ni²⁺ elution buffer (50 mM NaH₃PO₄, 300 mM NaCl, 250 mM imidazole, pH adjusted to 8.0 with NaOH). The eluted sample was dialyzed for 4 hours in storage buffer (20 mM Tris-HCl, pH 7.5, 50 mM NaCl, 1 mM DTT) using the SnakeSkin dialysis membrane (Thermo Scientific). Dialyzed proteins were clarified by centrifugation at 3,000 rpm, 30 min, 4°C. Clarified samples were concentrated using a 10 kDa molecular weight cut-off Vivaspin 20 concentrator (GE Healthcare). Purified proteins were frozen with liquid nitrogen and stored at -80°C.

Lipid binding cosedimentation assays

Lipids from the following sources were purchased from Avanti Polar Lipids: 1,2-dioleoyl-sn-glycero-3-phosphocholine, 1,2-Dioleoyl-sn-Glycero-3-[Phospho-L-Serine], L- (Egg,

Chicken), L- α -Phosphatidylinositol-4-phosphate (Brain, Porcine), L- α - α -Phosphatidic acid (Egg, chicken), Phosphatidylinositol-4,5-bisphosphate (Brain, Porcine), and 1,2-dioleoyl-sn-glycero-3-[phosphoinositol-3,4,5-trisphosphate]. Giant unilamellar vesicles were prepared as described (Winters et al., 2005). Briefly, lipids were added to chloroform at the molar ratios specified, chloroform was removed by rotovap and placing under vacuum for 15 min. Giant unilamellar vesicles were formed by resuspending in 0.2 M sucrose at 0.5 mg/mL total lipid by incubation at 50°C for 4 hours or overnight. Vesicles were stored at 4°C and used within 3 days of generation.

Pelleting assays were performed as previously described (Prehoda et al., 2000). For pelleting assay without aPKC, proteins were pre-spun to clarify in TLA-100 rotor, 65,000 rpm, 20 min, 4°C. All lipid binding cosedimentation assays contained 1-6 μ M MBP-tagged protein and 0.23 mg/mL total lipid in assay buffer (20 mM HEPES, pH 7.5, 50 mM NaCl, 1 mM DTT). After incubating proteins and vesicles at 30°C for 30 min, samples were pelleted by ultracentrifugation in a TLA-100 rotor at 65,000 rpm, 60 min, 4°C. The supernatants were removed, the pellets were washed, then the pellets were resuspended in a volume equal to the reaction volume. All samples were run on a 12.5% SDS-PAGE gel and stained with Coomassie Brilliant Blue for analysis. Gels were imaged using a scanner or the LiCOR. The band intensities were quantified using LiCOR ImageStudio and ImageJ. Gel images were processed with ImageJ and the Adobe Suite.

All pelleting assays containing aPKC were performed essentially as described above with the changes noted below. Reactions contained 0.1-0.5 μ M MBP-tagged proteins and 0.034 μ M aPKC in reaction buffer (500 mM Tris-HCl, pH 7.5, 100 mM NaCl, 100 μ M ATP, 100 μ M MgCl₂). Immunoblotting was performed to detect protein using mouse anti-MBP (1:1000, Santa Cruz Biotechnologies) and IRDye 800 CW goat anti-mouse (1:10,000, LiCOR). Membranes were blocked with TBS-T with 3% milk. Membranes were imaged with using a LiCOR and images were processed with the Adobe Suite. Band intensities were quantified with LiCOR ImageStudio and band intensity data was analyzed using Prism.

Protein kinase assays

Kinase assays were performed as previously described (Atwood and Prehoda, 2009; Graybill et al., 2012). Briefly, aPKC and substrates were incubated in assay buffer (50 mM Tris-HCl, pH 7.5, 100 mM NaCl, 10 mM MgCl₂) at 30°C for 5 min before addition of 1 mM ATP doped with [γ -³²P]ATP (~1.0 X 10⁵/nmol of ATP). The kinase reaction proceeded for 30 minutes before it was quenched by SDS loading dye. Samples were run on a 12.5% acrylamide SDS-PAGE gel, were dried, and exposed to a phosphor screen (Molecular Dynamics). The phosphor screen was imaged with a Storm 860. Images from the Storm 860 Molecular Imager were processed with ImageJ and the Adobe Suite.

Computational identification of PRBH motifs

The PRBH algorithm was implemented using the Python programming language with standard Python libraries including numpy and matplotlib. EMBL-EBI reference proteome files from *Homo sapiens*, *D. melanogaster*, *C. elegans*, and *S. cerevisiae*. The BH scoring algorithm used the previously described scores for BH character (Brzeska et al., 2010): A, -0.17; C, 0.24; D, -1.23; E, -2.02; F, 1.13; G, -0.01; H, -0.17; I, 0.31; K, 2; L, 0.56; M, 0.23; N, -0.42; P, -0.45; Q, -0.58; R, 2; S, -0.13; T, -0.14; V, -0.07; W, 1.85; Y, 0.94. Each amino acid residue was assigned a BH score for over a 19 residue BH window (i.e. the amino acid and its 9 NH₂- and COOH-terminal neighbors; unless specified otherwise). Sequences of adjacent residues with BH scores over a BH threshold of 0.6 were identified as peaks. The amino acid sequence of the peak, as well as, the maximum BH score and area over the BH threshold were compiled in a peak list. For human Numb and CKI γ -2, the BH window was reduced to 15 residues such that BH motifs at the extreme NH₂- and COOH-terminus were identified. BH scores for residues 9 residues or less from the NH₂- or COOH-terminus cannot be scored. Reducing the BH window allows residues closer to the NH₂- or COOH-terminus to be scored.

aPKC consensus sequences were identified by scoring the residues flanking S/T residues. The positional scoring was based on the previously described aPKC consensus sequence (Wang et al., 2012). This scoring metric does not strictly follow the consensus sequence from Wang and coworkers such that Ser 96, a verified aPKC

phosphosites on Mira, fit the consensus. Hydrophobic residues were score as follows, except where noted otherwise: A, 0.05; F, 0.2; I, 0.2; L, 0.2; M, 0.25; V, 0.1; W, 0.1; Y, 0.1. Basic residues were score as follows, except where noted otherwise: R, 0.1; K, 0.07; H, 0.04; D, -0.06; E, -0.06. Residues in the +2 position were scored as follows: R, 0.35; K, 0.15; H, 0.05. Residues in the +3 position were scored as follows: F, 0.25; L, 0.25; M, 0.25; I, 0.15; V, 0.1; W, 0.1; Y, 0.1; A, 0.05; R, 0.1; K, 0.1; H, 0.05. The +1 position was scored using the hydrophobic residue metric, and a penalty of -0.4 was given for residues that were not hydrophobic. Points were awarded for basic or hydrophobic residues from the -9 to the -4 position. Sequences with aPKC scores above the aPKC threshold of 0.6 were compiled in an aPKC site list. For proteins with multiple aPKC sites, each was included in the aPKC site list with its corresponding site score.

The aPKC site list and the BH site list were compared, and the PRBH algorithm analyzed sequences occurring in both lists. A PRBH score was computed for sequences occurring in both lists by using the following calculation: ‘Maximum BH score’ + ‘Maximum aPKC site score’ + 0.2 * ‘aPKC site number in the PRBH motif’. Three additional tests were performed on PRBH sequences: first, the area of the BH motif must be less than 400X the number of aPKC phosphosites. This eliminated many highly basic sequences with few candidate sites. Such sequences were not desired, as phosphorylation is not likely to alter BH character dramatically. Second, when a BH window size of 19 was used, BH motifs with areas less than 90 were discarded. This parameter was not used for identification of PRBH motifs at a protein’s NH₂- or COOH- terminus because the BH scoring metric reduces the BH signal for these peaks due to the scoring process. Third, PRBH scores less than the PRBH threshold of 1.6 were discarded. Sequences that passed these criteria were compiled in a PRBH sequence list that included the following: protein names, PRBH score, the PRBH sequence, maximum BH score, BH area, aPKC site scores, and aPKC site sequences.

The PRBH Motif Identification Program

```
#!/usr/bin/env python
```

```
class fasta:
    def __init__(self, desc, seq):
        self.f.desc = desc
        self.f.seq = seq

def fasta_file(it):
    """
    generator that returns an iterator over the records in a FASTA format file
    """
    d = fasta(' ', ' ')
    for i in it:
        if i[0] == '>':
            if len(d.seq) > 0:
                yield d
                d = fasta(' ', ' ')
            d.desc = i[1:].strip()
        else:
            d.seq += i.strip()
    if len(d.seq) > 0:
        yield d

hydRes = {'A': 0.05, 'F': 0.2, 'I': 0.2, 'L': 0.2, 'M': 0.25, 'V': 0.1, 'W': 0.1, 'Y': 0.1}
basicRes = {'R': 0.1, 'K': 0.07, 'H': 0.04, 'D': -0.06, 'E': -0.06, 'Y': 0.0}
M3Res =
{'F': 0.25, 'L': 0.25, 'M': 0.25, 'I': 0.15, 'V': 0.1, 'W': 0.1, 'Y': 0.1, 'A': 0.05, 'R': 0.1,
'K': 0.1, 'H': 0.05}
M2Res = {'R': 0.35, 'K': 0.15, 'H': 0.05}

class prbh_protein:
    def __init__(self, fasta, prbhs):
        self.f.fasta, self.f.prbhs = (fasta, prbhs)

class prbh_motif:
    def __init__(self, bh, apkcs, score):
        self.f.bh, self.f.apkcs, self.f.score = (bh, apkcs, score)
    def __eq__(self, other):
        return self.f.bh == other.bh and (self.f.score - other.score) < 0.00001 and
sel.f.apkcs[0] == other.apkcs[0]

class bh_motif:
    def __init__(self, start, end, height, area):
        self.f.start, self.f.end, self.f.height, self.f.area = (start, end, height, area)
    def __eq__(self, other):
        return self.f.start == other.start and (self.f.height - other.height) <
0.00001 and (self.f.area - other.area) < 0.00001

class aPKC_site:
    def __init__(self, pos, score, seq):
        self.f.pos, self.f.score, self.f.seq = (pos, score, seq)
    def __eq__(self, other):
        return self.f.pos == other.pos and (self.f.score - other.score) < 0.00001
and self.f.seq == other.seq

def max_seq(seq, score_dict):
    hyd = 0.0
    for i in seq:
        hyd = max(hyd, score_dict.get(i, 0.0))
    return hyd

def calc_aPKC_sites(seq, threshold=0.6):
    sites = []
    for pos, char in enumerate(str(seq).upper()):
        if char == 'S' or char == 'T':
            score = 0.0
            # pos + 1 hydrophobic
            if pos+1 < len(seq):
                score += hydRes.get(seq[pos+1], -0.4) # hydScore or -.4 if not
hydrophobic
            # pos +2 - +6 basic
```

```

basicTemp = 0.0
for i in range(2, 7):
    if pos+i+1 < len(seq):
        basicTemp += basicRes.get(seq[pos+i], 0.0)
score += basicTemp * 0.8
# pos -2 usually basic - very often arginine. -0.2 penalty if not
basic.
if pos-2 > 0:
    score += M2Res.get(seq[pos-2], 0.)*1.4
# pos -3: highest scoring hydrophobic, or basic residue with a
lower score. No penalty for others.
if pos-3 > 0:
    score += M3Res.get(seq[pos-3], 0.)
# pos -4 to -9: highest scoring basic and highest score
hydrophobic.
hyd = max_seq(seq[max(0, pos-9):max(0, pos-4)], hydRes)
bas = max_seq(seq[max(0, pos-9):max(0, pos-4)], basicRes)
score += (hyd + bas) * 0.5
if score > threshold:
    sites.append(APKC_sites(pos, score, seq[max(0, pos-
7):min(pos+17, len(seq))]))
return sites

bhDict = {'O': -17, 'U': 0, 'X': 0, 'A': -17, 'C': 0.24, 'D': -1.23, 'E': -2.02,
'F': 1.13, 'G': -0.01, 'H': -17, 'I': 31, 'K': 2, 'L': 56, 'M': 23, 'N': -42, 'P': -45,
'Q': -58, 'R': 2, 'S': -13, 'T': -14, 'V': -0.07, 'W': 1.85, 'Y': 94}

def running_bh_sum(seq, window_size):
    pos = 0
    if len(seq) < window_size:
        return
    running_sum = sum([bhDict.get(x, 0) for x in seq[:window_size]])
    yield running_sum
    for c in seq[window_size:]:
        running_sum += bhDict.get(c, 0) - bhDict.get(seq[pos], 0)
        pos += 1
        yield running_sum

def calc_bh(seq, window_size=19, threshold=0.6):
    motifs = []
    height = 0.0
    area = 0.0
    startRes = -1

    for pos, bsum in enumerate(running_bh_sum(seq, window_size)):
        bh_score = bsum/window_size
        if bh_score > threshold:
            if startRes == -1: #new BH
                startRes = pos
            height = max(bh_score, height)
            area += bsum
        elif startRes != -1: #close out BH
            motifs.append(bh_motif(startRes, pos+window_size, height, area))
            startRes = -1
            height = 0.0
            area = 0.0
    return motifs

def calc_bh_score(seq, window_size=19):
    scores = []
    for pos, bsum in enumerate(running_bh_sum(seq, window_size)):
        bh_score = bsum/window_size
        scores.append(bh_score)
    return scores

def calc_prbh(seq, threshold=1.6):
    prbhs = []
    bhs = []
    sites = calc_aPKC_sites(seq)
    if sites:
        bhs = calc_bh(seq)
    for bh in bhs:

```

```

phos = []
for apkc in sites:
    if apkc.pos > bh.start and apkc.pos < bh.end:
        phos.append(apkc)
if len(phos):
    score = bh.height + max([x.score for x in phos]) + len(phos)*0.2
    if bh.area < len(phos) * 400.:
        if bh.area/90. > 1:
            if score > threshold:
                prbhs.append(prbh_motif(bh, phos, score))
return prbhs

class tagged_prbh(object):
    def __init__(self, prbh, fasta):
        self.prbh, self.fasta = (prbh, fasta)
    def __eq__(self, other):
        return self.prbh.score - other.prbh.score < 0.00001 and
        self.prbh.apkcs[0].seq == other.prbh.apkcs[0].seq
    def __hash__(self):
        return hash((self.prbh.score, self.prbh.apkcs[0].seq))

def fasta_prbh(fasta):
    import gzip
    if fasta[-2:] == 'gz':
        fi = gzip.GzipFile(fasta, 'r')
    else:
        fi = open(fasta, 'r')

    hits = []
    with fi as f:
        for rec in fasta_file(f):
            prbhs = calc_prbh(rec.seq)
            for i in prbhs:
                hits.append(tagged_prbh(i, rec))
    return hits

def bh_motifs_string(seq, motifs):
    hit_string = list('*'*len(seq))
    motif_string = ""
    for a in motifs:
        width = a.end - a.start
        motif_string += ' '* (a.start - len(motif_string))
        motif_string += "{:>{width}}".format("{:.1f}".format(a.height))
    return motif_string

def apkc_sites_strings(seq, sites):
    hit_string = list('*'*len(seq))
    score_string = list(' '*len(seq))
    for a in sites:
        hit_string[a.pos] = '|'
    hit_string = ''.join(hit_string)
    for a in sites:
        s = "{:.1f}".format(a.score)
        score_string = score_string[:a.pos-1]+list(s)+list(' '* (len(seq)-
a.pos+1-len(s))) #score_string[a.pos-1+len(s):-len(s)+2]
        score_string = ''.join(score_string)
    return hit_string, score_string

human = fasta_prbh('/Path_to_input_file/9606.fasta.gz')
fly = fasta_prbh('/Path_to_input_file/7227.fasta.gz')
worm = fasta_prbh('/Path_to_input_file/6239.fasta.gz')
sponge = fasta_prbh('/Path_to_input_file/Amphimedon_queenslandica.Aqu1.26.pep.all.fa')
with_name = ((human, "human"), (fly, "fly"), (worm, "worm"), (sponge, "sponge"))

def max_site(apkcs):
    maxs = 0.0
    for i in apkcs:
        maxs = max(maxs, i.score)
    return maxs

```

```

human_s = sorted(human, key=lambda rec: rec.prbh.score, reverse=True)
fly_s = sorted(fly, key=lambda rec: rec.prbh.score, reverse=True)
worm_s = sorted(worm, key=lambda rec: rec.prbh.score, reverse=True)
sponge_s = sorted(sponge, key=lambda rec: rec.prbh.score, reverse=True)

sorted_prbh = (human_s, fly_s, worm_s, sponge_s)
with open('/File_for_results.txt', 'w+') as f1:
    for k in sorted_prbh:
        for i in k:
            s = ''
            for j in i.prbh.apkcs:
                s += "{}*{}*".format(j.score, j.seq)
            print
>>f1, '*', i.fasta.desc.split('|')[2], '*', i.prbh.score, '*', i.prbh.bh.area, '*', i.prbh.bh.height, '*', i.fasta.seq[i.prbh.bh.start:i.prbh.bh.end], '*', len(i.prbh.apkcs), '*', s

```

Supplemental References

- Atwood, S.X., and Prehoda, K.E. (2009). aPKC phosphorylates Miranda to polarize fate determinants during neuroblast asymmetric cell division. *Curr. Biol.* *19*, 723–729.
- Brzeska, H., Guag, J., Remmert, K., Chacko, S., and Korn, E.D. (2010). An experimentally based computer search identifies unstructured membrane-binding sites in proteins: application to class I myosins, PAKS, and CARMIL. *J. Biol. Chem.* *285*, 5738–5747.
- Graybill, C., Wee, B., Atwood, S.X., and Prehoda, K.E. (2012). Partitioning-defective Protein 6 (Par-6) Activates Atypical Protein Kinase C (aPKC) by Pseudosubstrate Displacement. *J. Biol. Chem.* *287*, 21003–21011.
- Lu, M.S., and Prehoda, K.E. (2013). A NudE/14-3-3 pathway coordinates dynein and the kinesin Khc73 to position the mitotic spindle. *Dev. Cell* *26*, 369–380.
- Prehoda, K.E., Scott, J.A., Mullins, R.D., and Lim, W.A. (2000). Integration of multiple signals through cooperative regulation of the N-WASP-Arp2/3 complex. *Science* *290*, 801–806.
- Wang, C., Shang, Y., Yu, J., and Zhang, M. (2012). Substrate recognition mechanism of atypical protein kinase Cs revealed by the structure of PKC ζ in complex with a substrate peptide from Par-3. *Struct. Lond. Engl.* *1993* *20*, 791–801.
- Winters, M.J., Lamson, R.E., Nakanishi, H., Neiman, A.M., and Pryciak, P.M. (2005). A membrane binding domain in the ste5 scaffold synergizes with gbetagamma binding to control localization and signaling in pheromone response. *Mol. Cell* *20*, 21–32.

Supplemental Data Table 1 (filename: “Supplemental Data Table 1.xlsx”). PRBH scores and descriptions. Related to Figure 5 and Supplemental Figure 4.

Supplemental Data Tables 1A-D list the PRBH motifs identified in the proteomes of human, fly, worm, and sponge, respectively. The PRBH score, maximum BH score, aPKC site scores, aPKC site sequences, and PRBH sequence also are given for each PRBH motif.